

Mechanistic detail and modeling of d-limonene with ozone in a darkness

Sirakarn Leungsakul and Richard M Kamens*
Department of Environmental Sciences and Engineering,
CB#7431 Rosenau Hall, University of North Carolina at Chapel Hill.
Chapel Hill, North Carolina 27599-7431

Abstract

A semi-explicit mechanism of d-limonene was developed and tested against experimental results performed inside large outdoor chambers at the UNC facility. The model couples gas phase reactions with partitioning processes and possible reactions inside particles. Reaction products and aerosol mass from the model were compared against experimental data. The model illustrates well not only the ozonolysis reaction of d-limonene but also a reasonable prediction of the secondary aerosol mass production under different conditions. Both simulation and experimental results suggested that d-limonene ozonolysis generates a significant amount of OH, which can not be explained by the hydroperoxide channel alone. A major product, limononaldehyde, was identified as well as keto-limonene, keto-limononaldehyde, limononic acid and keto-limononic acid. Identified particle phase products account for about 10-60% of gravimetric particle mass. Simulation of gas and particle phase reaction products showed reasonable fits to experimental data. Model sensitivity was tested and discussed with respect to effects of temperature, humidity, water uptake, and reactant concentrations.

*Corresponding author e-mail address: kamens@unc.edu,
telephone: 919-966-5452, fax: 919-966-7911

Introduction

Globally monoterpenes are estimated to account for 11% of the 1150 Tg C annual natural volatile organic compound emission (1). In the United States, 55% or more of monoterpene emission is α - and β -pinene and d-limonene emitted by conifers and crops (2, 3). Andersson-Sköld and Simpson (4) showed that terpenes may contribute as much as 2-50% of total organic aerosol, which can be greater than that from anthropogenic emission depending on location and season. While d-limonene may only represent 5-20% of the overall terpene emissions on mass basis, it may account for more than 20% of the terpene secondary aerosol material depending on the vegetative species distribution (4, 5). This reactivity makes d-limonene the second most important monoterpene from the perspective of aerosol formation potential. Thus if an aerosol mechanism is developed which includes α - and β -pinene, and d-limonene, one would be able to account for more than 50% of the biogenic aerosol formation under most circumstance. In addition, these three compounds structurally represent three different kinds of terpenes and can be generalized to include an evenly larger fraction of terpene emissions.

An ability to estimate the amount of particle formed yields several benefits. On the macro scale, the magnitude of global biogenic aerosol emissions impacts climate models because particles act directly as effective light absorption and light-backscattering objects (6, 7), which reflect incoming solar radiation, trap terrestrial infrared radiation (heat), and reduce visibility (8). They also act indirectly as cloud condensation nuclei (9, 10).

On a micro scale, the indoor aerosol potential of terpene reactions, and the resulting fine particles pose possible health risks (11-14). Terpenes, particularly d-limonene and α -pinene, are major components of essential oils from many types of vegetation. These

essential oils have been used as components of household products such as wood surface finishing, liquid cleaning agents, insect repellents and air fresheners, which can react with ozone and other radicals to form indoor aerosols (15–19).

In contrast to α - and β -pinene, there are few papers identifying and describing the mechanism of d-limonene reaction products (20–24). This paper presents a kinetic mechanism for the prediction of SOA from the reaction of d-limonene based on outdoor smog chamber experiments.

Experimental Section

Experiments were carried out either in a single 190m³ or dual 135 m³ outdoor Teflon film chambers located in Pittsboro, North Carolina. Chamber description were outlined elsewhere (for a single 190m³ chamber see 25, 26, for dual 135 m³ chambers see 27). Prior to experiments, the chambers were flushed with rural background air for 12 - 24 hours and dehumidified if necessary (28).

d-limonene + O₃ experiments were performed under darkness to preclude photochemical reactions. A known amount of d-limonene (97%, Aldrich, Milwaukee, WI) was first injected into the chamber to establish a desired concentration. Then ozone (O₃) was injected while the internal mixing fans were running. Ozone was measured with a Bendix chemiluminescent ozone meter (model 8002, Bendix Corp., Roncerverte, WV) or UV photometric ozone analyzer (model 49P/S, Thermo-Environmental Instruments, Indianapolis, IN). The instruments were calibrated by gas phase titration with a NIST traceable NO tank. Gas phase concentrations of d-limonene were measured by gas chromatography with flame ionization detection, GC-FID (Shimadzu, Japan, 1.5m×3.2mm ID Supelco5% Bentanone34 packed column). The GC-FID was calibrated against a NIST traceable hydrocarbon standard

tank. Aerosol data including particle size distribution was scanned every five to ten minutes using a Diffusion Mobility Analyzer and a Condensation Nuclei Counter (model SMPS 3936, TSI, St. Paul, MN). Aerosol mass was collected on filters as described in the sample collection section. Chamber temperature was measured with a temperature probe equipped with gill aspirated radiation shield (R.M. Young Company, Traverse City, MI) positioned inside the chamber. Dew point was measured either with a dew point hygrometer (model 800, EG&G, Waltham, MA) or with a relative humidity analyzer (model RH-100, Sable Systems, Las Vegas, NV). Chamber dilution rate was measured by monitoring the disappearance of SF₆, an inert gas, using a 6mm o.d. × 20 mm stainless steel molecular sieve column (50-80 mesh) and electron capture detector (PDD D-5, Valco Instruments Co. Inc., Houston, TX).

Sample collection and workup procedure

Gas and particle phase products were collected using a sampling train consisting of a two-stage 47mm Teflon-impregnated glass fiber filter (type T60A20, Pallflex Product Corp., Putnam, CT), followed by a 40-cm 5-channel denuder (University Research Glassware, Chapel Hill, NC) coated with XAD-4 (29). The sample was drawn from the chamber through the sampling train with a flow rate of 20 l/min. A backup filter was used to correct the amount of gas adsorbed onto the first filter (30). The filter was weighed before and after sampling for aerosol mass, and then spiked with internal standard, stored in an amber glass jar at 4°C and transported back to the UNC lab for extraction. The denuder was spiked with an internal standard, rinsed three times with methylene chloride (Optima grade, Fisher Scientific, Fair Lawn, NJ), and dried under a nitrogen stream before the next sampling (29).

The extracts were stored in a capped round bottom flask, covered with aluminum foil to prevent light exposure, and transported back to the UNC lab for analysis.

At the UNC lab, denuder extracts were concentrated to ~1 ml using rotary evaporation. The filter samples were extracted with methylene chloride by soxhlet extraction for 3 hrs. The filter extracts were concentrated to ~1 ml under a gentle nitrogen stream. The extracted samples were analyzed with Hewlet Packard (HP) 5890 Series II gas chromatograph (GC) (30m×0.25mm ID DB-5 capillary column, Supelco) equipped with HP5971A mass selective detector (MS). The temperature program was chosen to separate oxidation products. The injection temperature was 300 °C. Oven temperature was programmed at 60 °C for 1 minute, then ramped to 280 °C at the rate of 10 °C/min and maintained at 280 °C for 20 minutes. MS transfer line temperature was 310 °C.

Mechanistic Details

The d-limonene mechanism was constructed from gas-phase reactions to describe the initial reactivity of d-limonene with atmospheric oxidants. These reactions produce low vapor pressure compounds, which could partition between gas and condensed phases. A kinetic partitioning approach suggested by Kamens (31, 32) was used to describe time-dependent phase distribution during the reaction.

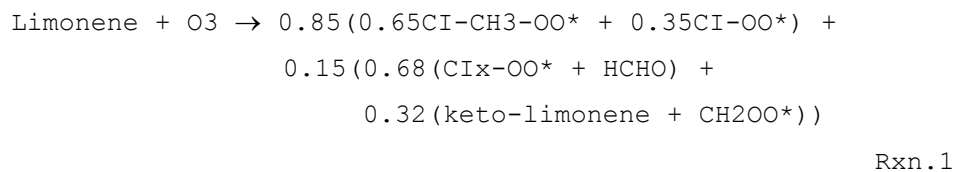
Mechanistic details were developed from literature and experimental data. Where no experimental data was available, gas phase kinetic parameters were calculated using structure reactivity relationship (33), the Master Chemical Mechanism (MCM) development protocol (34), or data from compounds of similar structure (35, 36). The d-limonene reactions were associated with the latest generation of the inorganic chemistry represented in the Carbon

Bond 4 photochemical smog mechanism, CB4_2003 (37). A kinetic solver called MORPHO developed by Jeffries (38) was used to perform the model simulations.

O₃ chemistry

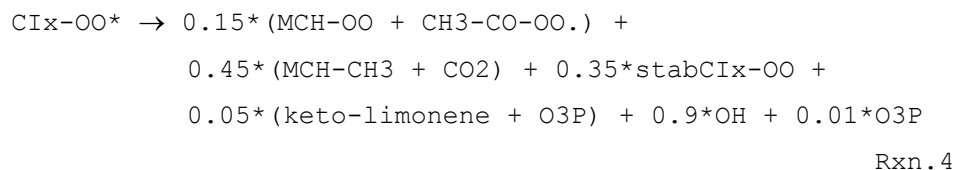
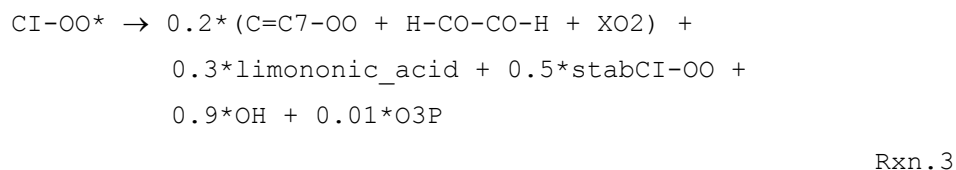
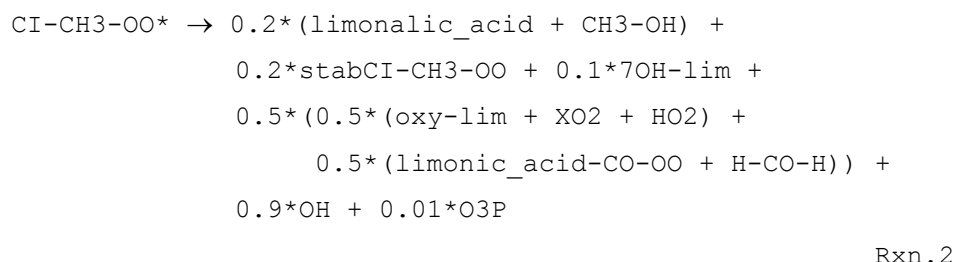
Only a few studies (20, 22) are available in the literature that can be used for mechanism development of the d-limonene and ozone reaction system. Very little product information is presented in these studies and, therefore, product analysis of similar compounds, i.e., cyclohexene, 1-methyl cyclohexene, and 1,2-dimethyl cyclohexene was used as a guide.

Initial O₃ attack on d-limonene can take place at either the internal cyclo double bonded carbon or at the external “iso-propylene” bond. The resulting ozonides produce four Criegee Intermediates (CIs) as shown in scheme I. The two CIs which result from O₃ attack on the cyclo double bond of d-limonene are called CI-CH₃-OO and CI-OO and still retain an external carbon double bond. The third CI, CIx-OO, retains the methyl cyclohexene structure from O₃ attack in the external carbon bond, and a fourth CI from this attack give the same one carbon CI formed from O₃ attack on ethylene, CH₂OO. This sequence is given below in Rxn. 1.



A ratio for O₃ attack on an internal cyclohexene carbon double bond compared to O₃ attack on an external carbon double bond of 2-hexene can be derived from their respective rate constants (36) and their observed products (21). For d-limonene a value of 85:15 for ozone attack on the endo- and exo-double bonded carbons gave the best fit to our

experimental data. For the CIs formed from the endo cyclic O₃ attack, a 65:35 split for internal CIs was assigned as per Atkinson's (36) recommendation for the α-pinene product distribution (39, 40). A split of external CIs was based on 2,3-dimethyl-1-butene, 2-methyl-1-pentene, and β-pinene product distributions (35, 41). The splitting ratios were also adjusted slightly to give best fit to overall experimental results. Currently two literature reaction rate coefficients for d-limonene ozonolysis are available: one recommended by Shu and Atkinson (1994) (42) is 2.01×10^{-16} and another by Khamaganov and Hites (43) is $2.95 \times 10^{-15} \exp(-783/T)$. Both rates agree within 10% at 298K, and the temperature dependent rate was used. The Criegee reactions are illustrated in the Rxn 2 – 4 sequence. In this sequence XO₂ is a generalized radical that implicitly accounts for the oxidation of NO to NO₂ and RO₂ to RO, and is common to Carbon Bond 4 mechanisms. HO₂ is the hydroperoxy radical. Definitions for other abbreviations are given in a glossary at the end of the manuscript.

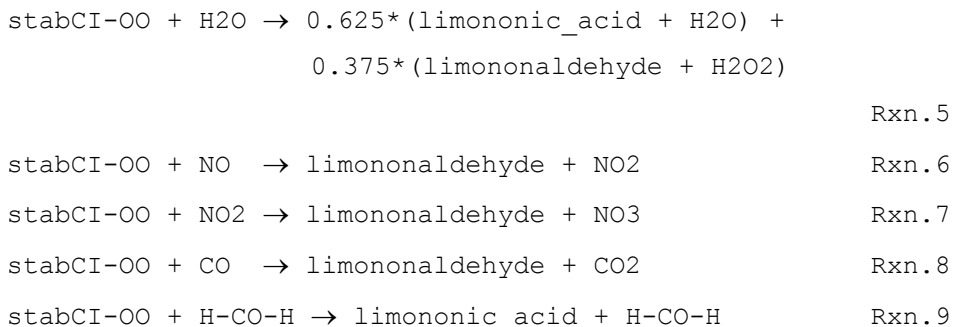


Currently, it is still uncertain how these CIs decompose. Studies suggested that these Criegee intermediates quickly rearrange, decompose, or thermally stabilize and then react

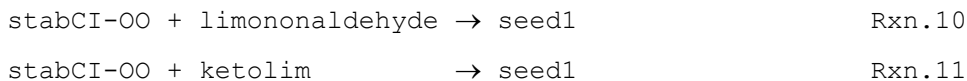
with other atmospheric constituents (34, 44–48) to form carbonyls, ketones, hydroxyl ketones, and carboxylic acids. Three major pathways represented in this mechanism are the hydroperoxy channel, the ester channel, and the stabilized CI channel (49). A choice has been made for reaction yield of each pathway due to lack of study in this area.

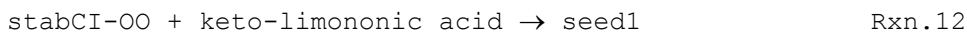
An overall OH molar yield of 86% with an error factor of 1.5 from ozonolysis of d-limonene has been reported (50, 51). This yield is slightly higher than the OH yield from the α -pinene system, which ranges from 0.75-0.85 (52, 53). In the simulation, an OH yield of 90% gave the best fit to observed d-limonene decay with O₃ in our chamber. To simulate a high OH yield without altering product distribution, OH was treated as being generated directly from all of the excited CI biradical decompositions (Rxn. 2 - 4).

Stabilized Criegee intermediates can react with number of compounds such as H₂O, NO, NO₂, CO, HCHO, HCOOH, and other aldehydes (48, 54, 55).



Evidence from direct mass spectrometry analysis of the condensed phase SOA (44, 56–58) strongly indicates that hydroperoxides, peroxyhemiacetals, and secondary ozonides were formed from reaction of stabilized CI in the presence of excess alcohols, carboxylic acids, aldehydes, and water vapor. These products were represented as “seed1” in the mechanism to allow lesser volatile species to partition onto these seed particles.



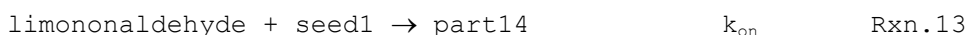


A reaction rate coefficient for the stabilized Criegee, CH₂OO with formaldehyde was reported to be in a range of 2×10^{-12} to 2×10^{-17} cm³/molecule-sec (46). A lower rate constant, 1.2×10^{-14} , for reaction of stabilized Criegee with carbonyls was used by Kamens and coworkers (31, 32) as recommended by Atkinson (36). This rate seems to give more reasonable results than the faster rate of Fenske (46). In our mechanism 99% of stabilized CIs react with water and less than 1% proceeds by reaction 10 – 12 to produce seed aerosol, which is sufficient to initiate particle growth. Recently, Ziemann (44) proposed that reaction of excited CIs generate low-volatility diacyl peroxides, which are responsible for seed nuclei formation.

Particle formation mechanism

In our chamber, d-limonene is first injected followed by an addition of ozone, a burst of particles is observed immediately when ozone was introduced. To simulate these instantaneous particle-phase products, the Criegee biradicals (Rxn.2 – 4) are rearranged and decomposed with a fast rate to readily formed low-vapor pressure products, i.e., limonic acid and limonic acid, and stabilized Criegee bi-radicals, stabCI-OO, which serve as seed precursor products (Rxn 10 – 12).

These immediate seed aerosols provide surface for more compounds to partition onto. The partitioning process employs kinetic rate constants for rates of absorption (k_{on}) from the gas to the particle phase and rates of desorption (k_{off}) from the particle phase to the gas phase (59). An example of limononaldehyde partitioning sequence is illustrated below in Rxn. 13 – 14.



part14 → limononaldehyde k_{off} Rxn.14

k_{off} was calculated from an inverse of the molecular vibrational frequency, $k_b T/h$, and its activated energy, E_a (60–64). E_a was estimated from vapor pressure as per Kamens (31).

$$k_{off} = \frac{k_b T}{h} \exp\left(\frac{-E_a}{RT}\right) \quad \text{Eq. 1}$$

At equilibrium, the ratio of k_{on} over k_{off} equals to the gas-particle partitioning equilibrium constant, K_P . With an assumption of equilibrium, theoretical k_{on} can be calculated from K_P and k_{off} . For liquid absorption, K_P can be calculated from theoretical considerations (65) as a function of liquid vapor pressure (p_L^0), temperature (T), and mean molecular weight of particle (MW_{om}) and this permits an estimate of k_{on} .

$$K_P = \frac{7.501RTf_{om}}{10^9 MW_{om} p_L^0 \gamma_{om}} \quad \text{Eq. 2}$$

$$k_{on} = K_P \times k_{off} \quad \text{Eq. 3}$$

Because there is no measured vapor pressure information for many of d-limonene products, an estimated vapor pressure is used to determine the partitioning equilibrium constant, K_P , value of individual products. One of the standard techniques for estimating vapor pressures, p_L^0 , of non-polar and moderately-polar compounds was demonstrated by Mackay (66) as a function of the boiling point, T_b , and entropy of vaporization, ΔS , based on the Clausius-Clapeyron equation.

$$\ln p_L^0 = \frac{\Delta S}{R} \left[1.803 \left(\frac{T_b}{T} - 1 \right) - 0.803 \left(\frac{T_b}{T} \right) \right] \quad (atm) \quad \text{Eq. 4}$$

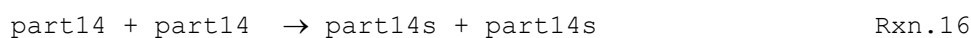
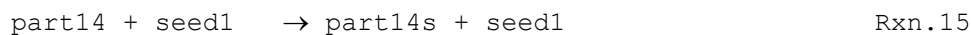
The normal boiling point was estimated using the Joback and Reid (67) extended group contribution method to cover more groups, and corrected for temperature-dependent

bias (68). The entropy of vaporization was computed based on group contribution (69) instead of using a constant value for all compounds.

Recently Jang (70) and Tolocka (71) provided evidence of acid catalyzed heterogeneous reactions of particle phase carbonyl compounds, which then lead to enhanced particle formation. Aldehydes in the particle phase can undergo polymerization to form dimers and trimers, i.e. C₂₀ to C₃₀ with estimated vapor pressures of 10⁻⁶ to 10⁻⁹ torr. This is considerably lower than estimated vapor pressure of the parent C₁₀ aldehydes, (2.3-7.5)×10⁻² torr.

This polymerization process upsets the partitioning equilibrium and drives additional gas-phase-aldehyde mass into the particle phase. The result is more particle mass. To represent this potential process, particle phase aldehydes are allowed to react to form more stable products that reside entirely in the particle phase.

Here for example, limonaldehyde in the particle phase (part14) reacts with the carbonyl portion associated with Criegee-secondary ozonides (seed1) to form a low vapor pressure compound composed of part14s +seed1. Since, however, the seed has additional carbonyl groups, it can undergo further aldol condensation or acetal reactions, in the mechanism it appears on the right side of the reaction. This makes it available for additional polymer growth.



Since the rate coefficients for these reactions are far from being quantified, they were set so the mass through this channel is low compared to the total SOA mass produced by the model.

Inorganic Mechanism

Two explicit inorganic mechanisms extracted from the 1999 version of the Carbon Bond mechanism (72), CB4_99, and from the 2003 version (37), CB4_2003, were added to d-limonene mechanism. Two major reactions have been updated in inorganic mechanism of CB4_2003 compared to CB4_99, these include an increased reaction rate constant of $\text{NO}_2 + \text{OH}$ to form HNO_3 , and an added reaction of N_2O_5 with H_2O . Other reaction rates were also updated with new literature values (37).

Simulation results showed that the nighttime d-limonene mechanism is insensitive to the changes made to inorganic mechanism from CB4_99 to CB4_2003. However, to keep the mechanism current, the new inorganic mechanism from CB_2003 was integrated into d-limonene mechanism.

Auxiliary Mechanism

To simulate chamber experiments, a UNC auxiliary wall mechanism was included. It accounts for physical properties and chemical reactivity based on the 150 m^3 UNC outdoor chamber and for sampling line reactions. Details of the auxiliary mechanism were described by Jeffries (73) and updated by Voicu (37). Since the wall model mainly affects radical sources and sinks involving oxides of nitrogen, it does not affect nighttime ozonolysis processes. Therefore, the main concern during the nighttime experiment is on ozone wall loss rate. As before, however, to keep the mechanism current, the new auxiliary wall model was implemented. The new 135 m^3 dual chambers were characterized for chamber reactivity. A limited number of characterized experiments were performed, which includes NO_x/O_3 decay, matched propylene with NO_x , matched particle, and particle wall loss experiments. Losses in the chamber due to exchange with the outside air are less than on

percent per hour. The average dark O₃ loss rate corrected for dilution was $7.53 \times 10^{-7} \text{ sec}^{-1}$ for the new 135 m³ chamber. A particle deposition was $1.16 \times 10^{-5} \text{ sec}^{-1}$ on a total mass basis.

The residence time of gas phase in the sample line was 1 second, which was used to correct a difference between observed and measured ozone and oxides of nitrogen concentrations due to reaction in the sample line.

Results and discussion

Experimental conditions

Nine experiments were conducted inside Teflon chambers and used for model simulation. Experimental conditions are shown in Table 1. Initial concentration ratio of d-limonene:ozone ranges from 0.8 – 4.2, which represent ozone excess and ozone deficit conditions. The lower concentration of d-limonene was limited by sensitivity of analytical techniques for product analysis.

Table 1: Experimental conditions aerosol yields of d-limonene + O₃ system.

Exp. Date	Initial concentration (ppm)		Temp (K)	DP (K)	ΔHC mg/m ³	ΔM_0 mg/m ³	Aerosol yield, Y ^d ($\Delta \text{M}_0 / \Delta \text{HC}$)
	d-limonene	O ₃					
18-Aug-99 ^{a,c}	0.63	0.3	297-302	293-296	2.172	1.378	0.634
10-Sep-99 ^a	0.18	0.12	292-298	287-290	0.594	0.403	0.678
1-Aug-01 ^a	0.65	0.81	288-292	288-289	3.589	3.385	0.943
13-Aug-03R ^{b,c}	0.48	0.18	295-302	295.4	2.348	1.814	0.773
13-Aug-03B ^{b,c}	0.45	0.35	295-302	295.6	2.371	1.855	0.782
22-Jan-04R ^b	0.093	0.022	277-274	269	0.505	0.128	0.427
22-Jan-04B ^b	0.093	0.081	277-274	269	0.300	0.228	0.451
23-Jan-04R ^b	0.296	0.251	269-270	264	1.644	1.190	0.724
23-Jan-04B ^b	0.143	0.239	269-270	264	0.848	0.653	0.770

(a) performed in 190 m³ chamber, (b) performed in 135 m³ dual chambers, R is North chamber and B is South chamber, (c) d-limonene was first injected followed by ozone. Reactions of d-limonene with background ozone were simulated to get initial conditions for particle mass, d-limonene, limononaldehyde, keto-limononaldehyde, and limonic acid, (d) aerosol yield was not corrected for dilution or losses.

Aerosol yield

Since experimental aerosol yield, Y , has been widely used as an indicator of aerosol forming potential (74–77), a maximum aerosol yield is calculated and reported in Table 1. The aerosol yield is defined as a ratio of amount of secondary organic aerosol formed, ΔM_0 , to the amount of reacted d-limonene, ΔHC . This aerosol yield has been linked to partitioning parameters using thermodynamic approach (74), which allows an estimation of aerosol mass contribution from each hydrocarbon. Although the thermodynamic approach is convenient and powerful, it does not yield product information nor can it account for an effect of humidity and reactions with other atmospheric constituents. As might be expected, the aerosol yields of d-limonene ozonolysis experiments performed inside UNC chambers are higher than the calculated yield using the two-parameter model of Griffin (76) from d-limonene photo-oxidation experiment.

An interesting comparison between aerosol yields of d-limonene and α -pinene ozonolysis systems (Table 1) shows d-limonene particle yields of 43 to 94 % and α -pinene particle yields of 18 to 67 % (31, 74, 75) with particle concentrations of 0.1 – 3.4 mg/m³ and 0.1 – 2.2 mg/m³, respectively. This difference illustrates a tremendous particle formation potential of d-limonene in the indoor environment (14–16, 78, 79) and the total particle formation of monoterpenes (4, 5).

Product analysis and identification

d-limonene products in gas and particle phases have been identified with GC-MS. A typical gas chromatogram is shown in Figure 1. d-limonene and limonene-oxide were identified with authentic standard. Limononaldehyde was synthesized (80) and confirmed by interpretation of Fourier transform infrared (FTIR), nuclear magnetic resonance (NMR) and GC-MS to have more than 95% purity. Keto-limononaldehyde, limononic acid, keto-limononic acid, 7OH-limononaldehyde, 7OH-keto-limononaldehyde, 7OH-limononic acid, and 7OH-keto-limononic acid were tentatively identified by their retention times and mass spectra. Some examples of product mass spectra are presented in Figure 2.

Limononaldehyde, the most significant primary product, was detected both in the gas phase and in the particle phase immediately after d-limonene was injected into the chamber. Keto-limononaldehyde, a secondary product appeared slightly later than limononaldehyde and was observed mostly in the particle phase. It forms from O₃ attack on the exterior carbon double bond of limononaldehyde. Limononaldehyde was the most abundant products in the gas phase and keto-limononaldehyde was the most abundant products in the particle phase. Identified products account for about 10 – 60% of total aerosol mass.

Evidence for particle phase reactions

In experiments performed for this study, background particle masses in the chamber at the beginning of an experiment were in the range of 0.3 – 4 µg/m³, therefore f_{om} after aerosol formation began was close to one. The products of d-limonene contain carbonyl, hydroxy, and carboxylic acid functional group. A five compound model UNIFAC calculation (81) gives an average γ_{om} of the products in a range of 1.2 – 1.32 (see discussion in Model Sensitivity section). From d-limonene product analysis, the MW_{om} was estimated

to range between 120 – 180 g/mol depending on humidity in the chamber (82 and later discussion). With these assumptions, K_p calculated at 298 K ranges from 1.3×10^{-3} to 1.7×10^{-3} m^3/mg and 5.9×10^{-3} to 7.7×10^{-3} m^3/mg for limononaldehyde and keto-limononaldehyde, respectively. As shown in Table 2 experimental K_p values are as much as two orders of magnitude higher than calculated K_p values. This finding is consistent with observed or apparent vapor pressures of product aldehydes from α -pinene oxidation (32), which are 1 – 2 orders of magnitudes lower than calculated theoretical values. Consistent with these observations is the FTIR spectrum of d-limonene particle phase products (Figure 3 and discussion in the particle phase reactions section). It suggests possible heterogeneous polymerization products, which is similar to the result from acidic seed-aldehyde experiments (70, 83, 84)

A possible explanation for all of the above observations that is consistent with other studies conducted by our group is the reaction of carbonyl compounds in particle phase to form larger molecules (70, 71, 84). This process drives the gas phase compounds to partition more into the particle phase. Analytically, some fraction of these oligomers may decompose back to original compounds during work-up procedures and are detected as their parent carbonyl compounds, hence the large deviation between observed K_p and predicted K_p values for aldehydes.

Table 2. Average values of experimental K_p in m^3/mg for limononaldehyde and keto-limononaldehyde.

Nighttime Exp. ID	Experimental K_p (m^3/mg)	
	limononaldehyde	keto-limononaldehyde
Au0101	0.0689	1.7564
Au1303R	0.0607	1.6685
Au1303B	0.0458	1.4052

$Experimental K_p = \frac{C_{part}}{C_{gas}[TSP]}$, $Predicted K_p = \frac{7.501RTf_{om}}{10^6 MW_{om} P_{L,om}^0}$. Predicted K_p of limononaldehyde = 0.0016 m³/mg,
predicted K_p of keto-limononaldehyde = 0.0071 m³/mg.

Simulation of d-limonene and ozone and aerosol mass

Simulation results (Figure 4) of d-limonene chemistry were very reasonable. The model predictions in some cases corresponded exactly with measured concentrations of d-limonene and ozone. Simulations of experiments on Aug 13, 2003 illustrate the model's ability to perform when d-limonene and ozone become excess. Although the model simulation results were very good when ozone was in excess over d-limonene, the fits for excess d-limonene were not as good, but still reasonable.

The model simulations predicted aerosol mass formation within 20% or better of measured gravimetric mass ranging between 0.4 -3.4 mg/m³. The model performs better for higher concentration runs, however, in a low ozone concentration experiment, the model yields a reasonable particle mass after the initial burst of particles formed in the chamber.

The heterogeneous rates used in the mechanism are assumed to be non-temperature dependent and the rates were extrapolated from particle phase to gas phase rates. Given that polymerization does occur in the bulk phase and pressure inside a small particle is larger than that of the bulk phase, it is reasonable to project that reaction occurs inside particle and the rate is faster than that in the bulk phase. Overall, polymerization reactions generally accounted for about 10% of the predicted simulation mass.

Gas – particle product distribution

The model can reasonably simulate limononaldehyde and keto-limononaldehyde in both gas and particle phases as showed in Figure 5. The differences between measured data and simulation may occur from (1) extraction and measurement procedures, which are harsh

techniques and may destroy or decompose long-chain products to some extent, (2) the model products represent not only themselves but also similar products. Since limited reaction products are preferred, similar products are combined together and represent as one.

Experimental time profiles of limononaldehyde indicate that limononaldehyde was generated initially and was consumed from both the gas and particle phases. This indicates that either (1) there is an exchange between gas and particle phases, or (2) they react further and form more stable products, or (3) their products do not decompose to original compounds during analysis.

Model sensitivity

Temperature

When particle production is dominated by seed production and heterogeneous reactions, the model is less sensitive to temperature in spite of a temperature dependent partitioning process. A pronounced temperature effect has been shown in α -pinene system (31, 32). It should be noted that Kamens α -pinene mechanism used a constant k_{on} rate coefficient, which leaves only k_{off} as temperature dependent. This use resulted in 25-30% total particle mass change over 10 degree K. In contrast, the d-limonene mechanism employed direct relationship between K_P and k_{on} . However this only makes a slight difference because k_{on} varies by square root of reciprocal of temperature. A more important parameter that has a direct effect on K_P value is vapor pressure, which is calculated in the model and is updated every time step to account for the temperature change.

Our experimental results (Table 1) show that aerosol yields from the d-limonene and ozone system tend to be lower as temperature decreases from 300 to 270 K (average

temperature). To simulate this behavior, the particle mass production from seed/SOZ is set to be lower than the temperature-dependent partitioning mass.

The temperature sensitivity test simulations were run at two ozone concentrations, 0.2 and 0.4 ppm of ozone with 0.4 ppm d-limonene at a dew point (DP) temperature of 283 K and temperature varied from 283 K to 313 K. Results showed that the lower ozone system is slightly more sensitive to temperature change. For every 10°C decrease, total aerosol mass increases about 16% and 10% for lower ozone and higher ozone systems, respectively. Product distribution for the lower ozone system is dominated by first generation product, mainly limonic acid, limonic acid, oxy-limononaldehyde and limononaldehyde. In the higher ozone system, secondary products, keto-limononaldehyde and hemiacetal were more significant. These secondary products have lower vapor pressures and tend to reside solely in particle phase, which in turn are less temperature dependent.

Humidity and water uptake

The model shows sensitivity to humidity change. At an initial condition of 0.4 ppm d-limonene and 0.2 ppm O₃ at 298 K, model predicted particle mass decreases by 10% from 0.8 to 0.72 mg/m³ as the dew point increases from 268 K to 298 K (13 – 100% RH). This result is supported by dry and humid experiments of stabilized Criegee radical reactions (45). Here, under normal atmospheric condition, a major pathway of stabilized CI is reaction with water to form carbonyls. Once water becomes limited, stabilized CI reacts with other constituents, in this case, aldehydes to form a less volatile compounds i.e., secondary ozonides, which increases the total mass.

Water uptake by SOA from α -pinene and ozone reaction reported by Jang and Kamens (82) can be up to 5% by mass at 100%RH. This uptake affects activity coefficients of condensed organic compounds and the average molecular mass of the particle.

As discussed earlier, humidity also has a reverse effect on particle formation by reacting with stabilized CIs, however, to assess the effect of water uptake by particles and eliminate influence of water reactions, a base case simulation was run at 298 K, 288 K dew point temperature, 0.4 ppm d-limonene and 0.2 ppm O₃. The base case was simulated to get a product distribution to estimate an average molecular mass, which did not include water uptake.

Table 3. Average molecular weight of particles and activity coefficient as a function of water uptake by particles.

Water uptake ¹ % by mass	Average MW _{om} ²	Average γ_{om} ³	MW _{om} × γ_{om}
0	179	1.2	215
1	164	1.23	202
2	152	1.24	188
3	142	1.27	180
4	133	1.29	172
5	126	1.32	166

(1) reported from α -pinene + O₃ dark experiment as ${}^wC_{om} \text{ (g/g)} = 5.2 \times 10^{-4} \times \%RH$ by Jang and Kamens (1998),
 (2) estimated from simulation result after reaching a maximum mass, conditions are described in the above text,
 (3) using 5 compound UNIFAC model : keto-limononaldehyde 35%, keto-limononic acid 35%, limonic acid 24%, SOZ 6%.

Average activity coefficients presented in Table 3 vary in a narrow range between 1.2 to 1.32, however, average molecular weight of the particles vary greatly from 179 to 126, which has more influence on K_P calculation (Table 2). The partitioning model uses K_P in a form of k_{on} (see Eq. 3) and has units of cm³/molecule-sec. In the transformation from m³/μg-sec to cm³/molecule-sec, the average MW_{om} cancels out in calculating k_{on} and k_{off}, which

leaves only the activity coefficient parameter. The UNIFAC calculation suggests that as water content in the particle increases, the activity coefficient of carboxylic acids decreases, but the activity coefficients of keto-aldehydes and Criegee type seeds slightly increase from one. Since this change is very small, however, an activity coefficient at a constant value of 1.27 at 3% water uptake by particle mass was assumed and this value is embedded in k_{on} value.

Reactant concentration

Influence of d-limonene concentration: To address this situation, simulations were run at constant initial ozone of 0.2 ppm, at a temperature of 298 K, and a dew point temperature of 283 K (40% RH). The d-limonene concentration was then varied between 10 ppb to 1.1 ppm. Results are shown in Table 4a. A maximum TSP is approached when the initial d-limonene:ozone ratio is about 2.5. At this ratio all of the O₃ is rapidly consumed and further gas phase reactions that generate SOA fall off rapidly.

Table 4a. Particle productions under different d-limonene concentration. Simulations were ran at 298 K, dew point temperature 283 K, and initial ozone of 0.2 ppm.

initial d-limonene (ppm)	ΔHC^a		ΔTSP_{max} (mg/m ³)	$Y_{max} = \Delta TSP_{max}/\Delta HC$	Initial d-limonene : O ₃ ratio
	(ppm)	(mg/m ³)			
0.01	0.010	0.055	0.021	0.378	0.05
0.05	0.050	0.276	0.113	0.410	0.25
0.10	0.100	0.551	0.235	0.428	0.5
0.30	0.266	1.471	0.694	0.472	1.5
0.50	0.348	1.921	0.783	0.408	2.5
0.70	0.364	2.009	0.779	0.388	3.5
0.90	0.375	2.071	0.777	0.375	4.5
1.10	0.382	2.108	0.778	0.369	5.5

(a) ΔHC is concentration of reacted d-limonene.

Influence of ozone concentration: Simulations were run at the same initial condition with 0.2 ppm d-limonene and varied O₃ from 10 ppb to 0.7 ppm. Results are shown in Table 4b. After d-limonene became limited, particle mass increases slightly as ozone increases and seems to approach some constant value after exhausted all reactive compounds.

Table 4b. Particle productions with different ozone concentrations. Simulation results were ran at 298 K, a dew point temperature of 283 K, and an initial d-limonene of 0.2 ppm.

initial ozone (ppm)	Δ HC		Δ TSP _{max} (mg/m ³)	Y _{max} = / Δ HC	Initial d-limonene : O ₃ ratio
	(ppm)	(mg/m ³)			
0.01	0.033	0.184	0.031	0.167	20
0.05	0.100	0.554	0.154	0.279	4
0.10	0.167	0.919	0.325	0.354	2
0.20	0.200	1.103	0.489	0.444	1
0.50	0.200	1.104	0.528	0.478	0.4
0.70	0.200	1.104	0.530	0.480	0.29

Particle phase reactions

FTIR spectrum of particles collected on ZnSe FTIR windows from a 5 ppm d-limonene + and 1 ppm O₃ system after 2.5 hours of reaction in the dark shows the appearance of C-O-C stretch band, suggesting possible polymerization in the 1000 cm⁻¹ region (Figure 3). At this stage it is not possible to quantify this process. When the process is not included in the model, the model tends to under predict observed particle concentrations by ~ 10% and hence we have attempted to include a first generation polymerization scheme in the mechanism.

A sensitivity test to the particle reaction rate constant was performed to assess an importance of the particle phase reaction. The conditions used are 0.3 ppm d-limonene, 0.2 ppm O₃, at 293 K, and a dew point temperature of 283 K. Without particle phase reactions,

the model yields maximum particle mass of 0.43 mg/m^3 . With a reverse particle phase reaction of 0.0001 sec^{-1} a limit of particle reaction rate constant is in a range of 1×10^{-15} to $\times 10^{-10} \text{ cm}^3/\text{molecule-sec}$. This range translates into a particle mass contribution of 2 to 55 % increase from the base case without particle phase reactions and is limited by the gas to particle partitioning rate. Although there is evidence of particle reaction, reactions presented in the model are used as adjusting parameter. By using a reaction rate of $8 \times 10^{-15} \text{ cm}^3/\text{molecule-sec}$ an average increase in particle mass about 12 % is observed.

Model simulation of other studies

Three sets of published experimental results were simulated with this d-limonene mechanism. Li and coworkers (79) performed experiments in an office setting. d-limonene and ozone were emitted in a closed door office with low and high air exchange rates. Sarwar and coworkers (15) experimented with different kinds of scented household products in a stainless steel (SS) chamber. These scented products, which contain d-limonene in different fractions were applied or released inside the chamber that has a certain level of ozone. Rohr and coworkers (17) used a flow reactor tube with a small plexiglass chamber attached to the end where samples were taken. A constant flow of d-limonene and ozone was introduced continuously.

Reactor characteristic parameters were adjusted to suit each setting. Particle wall loss rate constant in the office, SS chamber, and flow reactor were approximated to 1.2×10^{-4} , 1.2×10^{-4} , $2 \times 10^{-3} \text{ sec}^{-1}$, respectively. Entrained gas concentrations were assumed to be at background level, 10 ppb for office and 45 ppb for SS chamber. Because the office setting is not well characterized, average values of 15 and 2 hr^{-1} were used for high and low air exchange rates (AER). The d-limonene concentration of 270 ppb reported on 2/11/00

experiment without ozone generator was used to get an average emission rate of d-limonene from diffusion vessel. This rate was used for all low AER experiments except for experiment on 1/4/00, a higher rate was used to get a reported residual d-limonene of 360 ppb. For high AER experiments, emission rates of ozone and d-limonene were adjusted to get the reported net ozone and d-limonene concentrations. For the SS chamber, only the d-limonene fraction emitted from tested products was used to simulate the particle formation, all experiments were simulated as puff injection. In the flow reactor the reactants were injected continuously with a certain flow rate. Different AER affected the time required to reach steady state, which varies from 2 to 20 minutes. Experimental conditions of these three sets of experiments are summarized in Table 5. One feature of the model developed in this study is that it can be easily extended and applied to a flow reactor system. As demonstrated, the model is capable of predicting particle mass generated from different systems despite approximated chamber parameters for particle and ozone deposition rates.

Table 5. Simulation conditions used in the d-limonene model to simulate particle mass (PM) from different studies. Reported PM and predicted PM from the model are compared in the last two columns.

Exp. ID	O ₃ (ppb)	d-limonene (ppb)	Exp. Temp (°C)	RH (%)	AER ^a (hr ⁻¹)	Measured ^b PM (µg/m ³)	Predicted PM (µg/m ³)
Office – Li et al., 2002							
12/16/1999	125 ^c	160 ^d	21 ^e	10	15 ^f	17	68
12/29/1999	100 ^c	<1 ^d	21 ^e	9	15 ^f	0.2	0.01
1/13/2000	100 ^c	240 ^d	21 ^e	28	15 ^f	45	77
1/19/2000	100 ^c	210 ^d	21 ^e	5	15 ^f	12	78
1/27/2000	80 ^c	205 ^d	21 ^e	6	2 ^f	>350 ^g	364
2/4/2000	80 ^c	360 ^d	21 ^e	35	2 ^f	>350 ^g	456
2/11/2000	<2 ^c	270 ^d	21 ^e	20	2 ^f	4	5.2
2/15/2000	172 ^c	125 ^d	21 ^e	11	2 ^f	>350 ^g	479
2/16/2000	125 ^c	175 ^d	21 ^e	30	2 ^f	>350 ^g	396
SS Chamber – Sarwar et al., 2004							
1	126	347 ^h	24	20 ⁱ	0.66	203	247
3	112	169 ^h	24	20 ⁱ	0.62	110	141

5	95	11 ^h	24	20 ⁱ	0.79	16	7
7	219	18 ^h	24	20 ⁱ	0.71	70	20
10	15	9 ^h	24	20 ⁱ	0.83	1.9	2

Flow Tube – Rohr et al., 2003

A	94	30000	20	19	8.6	51	153
B	138	48000	21	15	8.7	100	230
C	2550	62000	34	33	36.0	9179	10232
D	2742	73000	23	54	45.0	8649	12319
E	3125	33000	27	51	8.4	11213	7446

(a) AER is air exchange rate, (b) reported particle mass converted from particle volume. Sarwar et al. (2004) used particle density of 1.2 g/cm³, Rohr et al. (2003) used particle density of 1 g/cm³, (c) net ozone measured during experiments, (d) average value measured with passive sample devices, (e) assumed constant room temperature at 21°C, (f) average AER reported as high rate (12 – 18 hr⁻¹) and low rate (0.5 – 4 hr⁻¹), (g) exceed instrument limit, (h) estimated d-limonene concentration calculated from maximum terpene concentration × d-limonene content, (i) assumed relative humidity at 20%.

Acknowledgments

This work is supported by a STAR grant from the U.S. EPA (R828176) to the University of North Carolina at Chapel Hill. Sirakarn Leungsakul receives a full scholarship from the Royal Thai Government for her study at the UNC-CH. We thank Bharadwaj Chandramouli, Nadine Czoschke, Di Hu, and Sangdon Lee for assisting with chamber experiments, Mohammed Jaoui for performing two experiments in 1999, Myoseon Jang for comments and assisting with FTIR sample and interpretation, and Ramiah Sangaiah for assisting with limononaldehyde synthesis and analysis.

Glossary

[CI-CH ₃ -OO]*	methyl-substituted excited Criegee intermediate from ozone reaction with internal double bond of d-limonene
[CI-OO]*	excited Criegee Intermediate from ozone reaction with d-limonene internal double bond
[CI _x -OO]*	excited Criegee Intermediate from ozone reaction with d-limonene external double bond
[CH ₂ OO]*	simplest Criegee intermediate from vinyl group
stabCI-OO	stabilized Criegee intermediate from ozone reaction with internal double bond of d-limonene

stabCI-CH3-OO	stabilized methyl-substituted Criegee intermediate from ozone reaction with internal double bond of d-limonene
stabCIx-OO	stabilized Criegee Intermediate from ozone reaction with d-limonene external double bond
CH3-CO-OO.	methyl peroxy radical
MCH-OO	1-methyl cyclohexene peroxy radical
C=C7-OO	C8 peroxy radical containing one double bond
limonic_acid-CO-OO	peroxy acyl radical, a precursor of limononic acid
O3P	ground-state singlet oxygen
OH	hydroxy radical
HCHO or H-CO-H	formaldehyde
CH3-OH	methanol
H-CO-CO-H	glyoxal
MCH-CH3	1-methyl cyclohexene
keto-limonene	limona ketone (4-acetyl-1-methylcyclohexene)
lim	limononaldehyde (3-isopropenyl-6-oxo-hetanal)
7OH-lim	7-hydroxy-limononaldehyde (3-isopropenyl-6-oxo-7-hydroxy-hetanal)
ketolim	keto-limononaldehyde (3-acetyl-6-oxo-heptanal)
keto-limononic acid	keto-limononic acid (3-acetyl-6-oxo-hetonoic acid)
oxy-lim	oxy-substituted limononaldehyde
seed1	low-vapor pressure nucleating products formed from stabilized Criegee intermediate reacting with product aldehydes and carboxylic acids
seed	initial background seed aerosol
part14	limononaldehyde in the particle phase
part14s	polymer product from limononaldehyde in the particle phase

Literature Cited

- (1) Guenther, A.; Hewitt, C. N.; Erickson, D.; Fall, R.; Geron, C.; Graedel, T.; Harley, P.; Klinger, L.; Lerdau, M.; et al *Journal of Geophysical Research, [Atmospheres]*

- 1995**, *100*, 8873-92.
- (2) Went, F. W. *Nature*. **1960**, *187* 641-643.
 - (3) Lamb, B.; Gay, D.; Westberg, H.; Pierce, T. *Atmospheric Environment, Part A: General Topics* **1993**, *27A*, 1673-90.
 - (4) Andersson-Skold, Y.; Simpson, D. *Journal of Geophysical Research, [Atmospheres]* **2001**, *106*, 7357-7374.
 - (5) Griffin, R. J.; Cocker, D. R. I.; Seinfeld, J. H.; Dabdub, D. *Geophysical Research Letters* **1999**, *26*, 2721-2724.
 - (6) Koloutsou-Vakakis, S.; Rood, M. J.; Nenes, A.; Pilinis, C. *Journal of Geophysical Research, [Atmospheres]* **1998**, *103*, 17009-17032.
 - (7) Molnar, A.; Meszaros, E. *Atmospheric Environment* **2001**, *35*, 5053-5058.
 - (8) Horvath, H. *Atmospheric Environment, Part A: General Topics* **1993**, *27A*, 293-317.
 - (9) Novakov, T.; Penner, J. E. *Nature (London, United Kingdom)* **1993**, *365*, 823-6.
 - (10) Charlson, R. J.; Schwartz, S. E.; Hales, J. M.; Cess, R. D.; Coakley, J. A. Jr.; Hansen, J. E.; Hofmann, D. J. *Science (Washington, DC, United States)* **1992**, *255*, 423-30.
 - (11) Rohr, A. C.; Wilkins, C. K.; Clausen, P. A.; Hammer, M.; Nielsen, G. D.; Wolkoff, P.; Spengler, J. D. *Inhalation Toxicology* **2002**, *14*, 663-84.
 - (12) Wolkoff, P.; Clausen, P. A.; Wilkins, C. K.; Nielsen, G. D. *Indoor Air* **2000**, *10*, 82-91.
 - (13) Clausen, P. A.; Wilkins, C. K.; Wolkoff, P.; Nielsen, G. D. *Environment International* **2001**, *26*, 511-522.
 - (14) Wainman, T.; Zhang, J.; Weschler, C. J.; Liroy, P. J. *Environmental Health Perspectives* **2000**, *108*, 1139-1145.
 - (15) Sarwar, G.; Olson, D. A.; Corsi, R. L.; Weschler, C. J. *Journal of the Air & Waste Management Association* **2004**, *54*, 367-377.
 - (16) Sarwar, G.; Corsi, R.; Allen, D.; Weschler, C. *Atmospheric Environment* **2003**, *37*, 1365-1381.

- (17) Rohr, A. C.; Weschler, C. J.; Koutrakis, P.; Spengler, J. D. *Aerosol Science and Technology* **2003**, *37*, 65-78.
- (18) Weschler, C. J.; Shields, H. C. *Atmospheric Environment* **1999**, *33*, 2301-2312.
- (19) Zhang, J.; Wilson, W. E.; Lioy, P. J. *Environmental Science and Technology* **1994**, *28*, 1975-82.
- (20) Grosjean, D.; Williams, E. L. I.; Seinfeld, J. H. *Environmental Science and Technology* **1992**, *26*, 1526-33.
- (21) Grosjean, D.; Williams, E. L. I.; Grosjean, E.; Andino, J. M.; Seinfeld, J. H. *Environmental Science and Technology* **1993**, *27*, 2754-8.
- (22) Calogirou, A.; Larsen, B. R.; Kotzias, D. *Atmospheric Environment* **1999**, *33*, 1423-1439.
- (23) Glasius, M.; Lahaniati, M.; Calogirou, A.; Di Bella, D.; Jensen, N. R.; Hjorth, J.; Kotzias, D.; Larsen, B. R. *Environmental Science and Technology* **2000**, *34*, 1001-1010.
- (24) Larsen, Bo. R.; Di Bella, D.; Glasius, M.; Winterhalter, R.; Jensen, N. R.; Hjorth, J. *Journal of Atmospheric Chemistry* **2001**, *38*, 231-276.
- (25) Fox, D. L.; Sickles, J. E.; Kuhlman, M. R.; Reist, P. C.; Wilson, W. E. *Journal of the Air Pollution Control Association* **1975**, *25*, 1049-53.
- (26) Kamens, R.; Odum, J.; Fan, Z.-H. *Environmental Science and Technology* **1995**, *29*, 43-50.
- (27) Lee, S.; Jang, M.; Kamens, R. M. *Atmospheric Environment* **2004**, *38*, 2597-2605.
- (28) Jaoui, M.; Kamens, R. M. *Journal of Geophysical Research, [Atmospheres]* **2001**, *106*, 12541-12558.
- (29) Fan, Z.; Chen, D.; Birla, P.; Kamens, R. M. *Atmospheric Environment* **1995**, *29*, 1171-81.
- (30) McDow, S. R.; Huntzicker, J. J. *Atmospheric Environment, Part A: General Topics* **1990**, *24A*, 2563-71.
- (31) Kamens, R.; Jang, M.; Chien, C.-J.; Leach, K. *Environmental Science and*

- Technology* **1999**, *33*, 1430-1438.
- (32) Kamens, R. M.; Jaoui, M. *Environmental Science and Technology* **2001**, *35*, 1394-1405.
- (33) Kwok, E. S. C.; Atkinson, R. *Atmospheric Environment* **1995**, *29*, 1685-95.
- (34) Jenkin, M. E.; Saunders, S. M.; Pilling, M. J. *Atmospheric Environment* **1997**, *31*, 81-104.
- (35) Calvert, J. G., Atkinson, R., Kerr, J. A., Madronich, S., Moortgat, G. K., Wallington, T. J., and Yarwood, G. *The Mechanisms of Atmospheric Oxidation of the Alkenes*. 502 pp. 1999.
- (36) Atkinson, R. *Journal of Physical and Chemical Reference Data* **1997**, *26*, 215-290.
- (37) Voicu, I. University of North Carolina at Chapel Hill, 2003.
- (38) Jeffries, Harvey, Kessler, Marc, and Gery, Michael. MComp/MEval: The Morphecule Reaction Mechanism Compiler/Solver Development and Testing of a New Photochemical Reaction Mechanism. *Last updated on 10/1/98. 02/12/2003.*
- (39) Noziere, B.; Barnes, I.; Becker, K.-H. *Journal of Geophysical Research, [Atmospheres]* **1999**, *104*, 23645-23656.
- (40) Warscheid, B.; Hoffmann, T. *Atmospheric Environment* **2001**, *35*, 2927-2940.
- (41) Winterhalter, R.; Neeb, P.; Grossmann, D.; Kolloff, A.; Horie, O.; Moortgat, G. *Journal of Atmospheric Chemistry* **2000**, *35*, 165-197.
- (42) Shu, Y.; Atkinson, R. *International Journal of Chemical Kinetics* **1994**, *26*, 1193-205.
- (43) Khamaganov, V. G.; Hites, R. A. *Journal of Physical Chemistry A* **2001**, *105*, 815-822.
- (44) Ziemann, P. J. *Journal of Physical Chemistry A* **2003**, *107*, 2048-2060.
- (45) Bonn, B.; Schuster, G.; Moortgat, G. K. *Journal of Physical Chemistry A* **2002**, *106*, 2869-2881.

- (46) Fenske, J. D.; Hasson, A. S.; Ho, A. W.; Paulson, S. E. *Journal of Physical Chemistry A* **2000**, *104*, 9921-9932.
- (47) Neeb, P.; Sauer, F.; Horie, O.; Moortgat, G. K. *Atmospheric Environment* **1997**, *31*, 1417-1423.
- (48) Neeb, P.; Horie, O.; Moortgat, G. K. *Tetrahedron Letters* **1996**, *37*, 9297-9300.
- (49) Finlayson-Pitts, B. J. and Pitts, J. N. *Chemistry of the Upper and Lower Atmosphere: Theory, Experiments, and Applications*. 1040 pp. 1999.
- (50) Paulson, S. E.; Chung, M. Y.; Hasson, A. S. *Journal of Physical Chemistry A* **1999**, *103*, 8125-8138.
- (51) Atkinson, R.; Hasegawa, D.; Aschmann, S. M. *International Journal of Chemical Kinetics* **1990**, *22*, 871-87.
- (52) Atkinson, R.; Aschmann, S. M.; Arey, J.; Shorees, B. *Journal of Geophysical Research, [Atmospheres]* **1992**, *97*, 6065-73.
- (53) Chew, A. A.; Atkinson, R. *Journal of Geophysical Research, [Atmospheres]* **1996**, *101*, 28649-28653.
- (54) Horie, O.; Neeb, P.; Moortgat, G. K. *International Journal of Chemical Kinetics* **1997**, *29*, 461-468.
- (55) Docherty, K. S.; Kumboonlert, K.; Lee, I. J.; Ziemann, P. J. *Journal of Chromatography, A* **2004**, *1029*, 205-215.
- (56) Ziemann, P. J.; Tobias, H. J.; Docherty, K. S. *Preprints of Extended Abstracts presented at the ACS National Meeting, American Chemical Society, Division of Environmental Chemistry* **2001**, *41*, 1219-1223.
- (57) Tobias, H. J.; Ziemann, P. J. *Journal of Physical Chemistry A* **2001**, *105*, 6129-6135.
- (58) Ziemann, P. J. *Journal of Physical Chemistry A* **2002**, *106*, 4390-4402.
- (59) Pankow, J. F. *Atmospheric Environment (1967-1989)* **1987**, *21*, 2275-83.
- (60) Glasstone, Samuel, Laidler, Keith J., and Eyring, Henry. *The Theory of Rate Processes. The Kinetics of Chemical Reactions, Viscosity, Diffusion and Electrochemical Phenomena*. 611 pp. 1941.

- (61) Yasuoka, K.; Matsumoto, M.; Kataoka, Y. *Journal of Chemical Physics* **1994**, *101*, 7904-11.
- (62) Matsumoto, M.; Yasuoka, K.; Kataoka, Y. *Journal of Chemical Physics* **1994**, *101*, 7912-17.
- (63) Donaldson, D. J. *Journal of Physical Chemistry A* **1999**, *103*, 62-70.
- (64) Donaldson, D. J.; Anderson, D. *Journal of Physical Chemistry A* **1999**, *103*, 871-876.
- (65) Pankow, J. F. *Atmospheric Environment* **1994**, *28*, 189-93.
- (66) Mackay, D.; Bobra, A.; Chan, D. W.; Shiu, W. Y. *Environ. Sci. Technol.* **1982**, *16* 645-649.
- (67) Joback, K. G.; Reid, R. C. *Chem. Eng. Commun.* **1987**, *57* (1-6), 233-243.
- (68) Stein, S. E.; Brown, R. L. *J.Chem. Inf. Comput. Sci.* **1994**, *34* 581-587.
- (69) Zhao, L.; Li, P.; Yalkowsky, S. H. *Journal of Chemical Information and Computer Sciences.* **1999**, *39* 1112-1116.
- (70) Jang, M.; Czoschke, N. M.; Lee, S.; Kamens, R. M. *Science* **2002**, *298*, 814-7.
- (71) Tolocka, M. P.; Jang, M.; Ginter, J. M.; Cox, F. J.; Kamens, R. M.; Johnston, M. V. *Environmental Science and Technology* **2004**, *38*, 1428-1434.
- (72) Adelman Z. E. University of North Carolina at Chapel Hill, 1999.
- (73) Jeffries, H.; Sexton, K.; Adelman, Z. *Auxiliary mechanisms (wall models) for UNC outdoor chamber*; EPA/600/R-00/076, Proceedings Sixth US/Germany Workshop on Ozone/Fine Particle Science, 1999;
- (74) Odum, J. R.; Hoffmann, T.; Bowman, F.; Collins, D.; Flagan, R. C.; Seinfeld, J. H. *Environmental Science and Technology* **1996**, *30*, 2580-2585.
- (75) Hoffmann, T.; Odum, J. R.; Bowman, F.; Collins, D.; Klockow, D.; Flagan, R. C.; Seinfeld, J. H. *Journal of Atmospheric Chemistry* **1997**, *26*, 189-222.
- (76) Griffin, R. J.; Cocker, D. R. I.; Flagan, R. C.; Seinfeld, J. H. *Journal of Geophysical Research, [Atmospheres]* **1999**, *104*, 3555-3567.

- (77) Pankow, J. F.; Seinfeld, J. H.; Asher, W. E.; Erdakos, G. B. *Environmental Science and Technology* **2001**, *35*, 1164-1172.
- (78) Fan, Z. ; Lioy, P.; Weschler, C.; Fiedler, N.; Kipen, H.; Zhang, J. *Environmental science & technology* **2003**, *37*, 1811-21.
- (79) Li Tsung-Hung; Turpin Barbara J; Shields Helen C; Weschler Charles J *Environmental science & technology* **2002**, *36*, 3295-302.
- (80) Wolinsky, J.; Barker, W. *Journal of the American Chemical Society* **1960**, *82*, 636-8.
- (81) Choy, B. and Reible, D. D. UNIFAC Activity coefficient Calculator Version 3.0. September, 1996.
- (82) Jang, M.; Kamens, R. M. *Environmental Science and Technology* **1998**, *32*, 1237-1243.
- (83) Jang, M.; Lee, S.; Kamens, R. M. *Atmospheric Environment* **2003**, *37*, 2125-2138.
- (84) Jang, M.; Kamens, R. M. *Environmental Science and Technology* **2001**, *35*, 4758-4766.

List of Figures

Figure 1. Gas chromatogram of d-limonene+O₃ products in (I) particle phase and (II) gas phase on Aug 13, 03. Mass spectra of tentatively identified products are shown.

Figure 2. Mass spectrum of particle phase products from d-limonene and ozone reactions.

Figure 3. FTIR spectra of d-limonene reaction products with ozone comparing with those of limonene diol and limononaldehyde standards.

Figure 4. Model simulations (lines) vs experimental data (symbols) for d-limonene with ozone experiments. LDT is local daylight-saving time. Thick line (—) is simulated ozone, dash line (- · -) is simulated d-limonene, line (—) is simulated aerosol, diamond (◇) is measured ozone, cross mark (×) is measured d-limonene, solid square (■) is measured aerosol.

Figure 5. Simulations (lines) vs data (symbols) of (a) limononaldehyde and (b) keto-limononaldehyde in gas and particle phases from Aug 13, 2003 B experiment.

Scheme I. d-limonene + O₃ reaction pathway for model products and product yields.

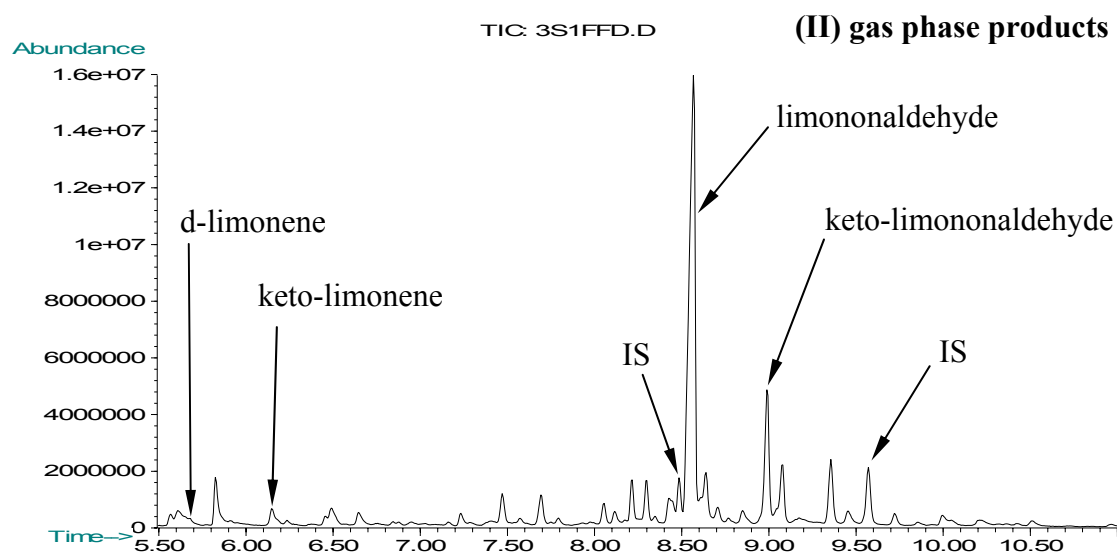
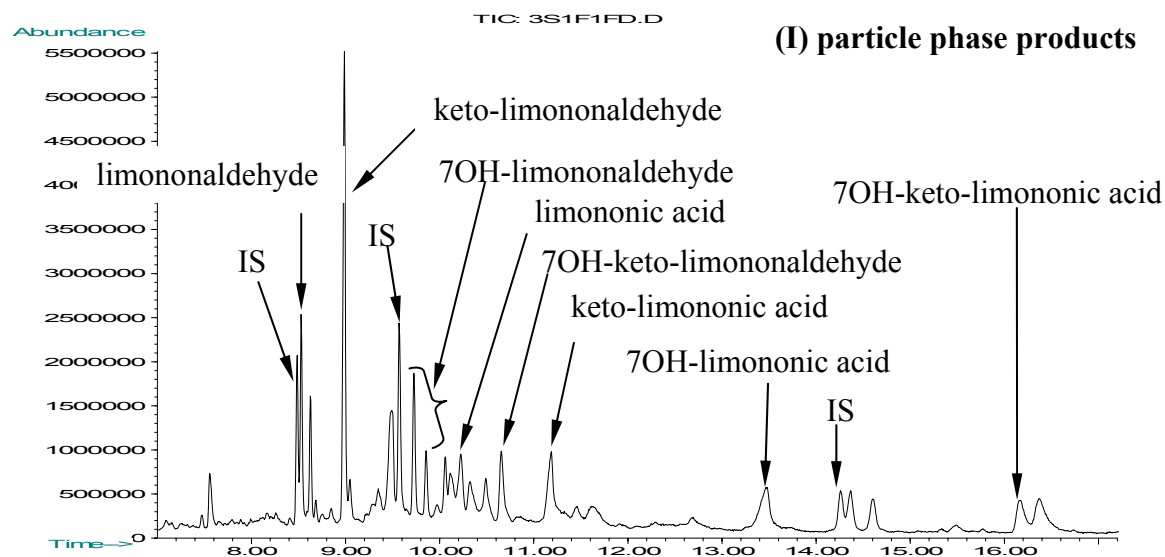


Figure 1. Gas chromatogram of d-limonene+O₃ products in (I) particle phase and (II) gas phase on Aug 13, 03. Mass spectra of tentatively identified products are shown.

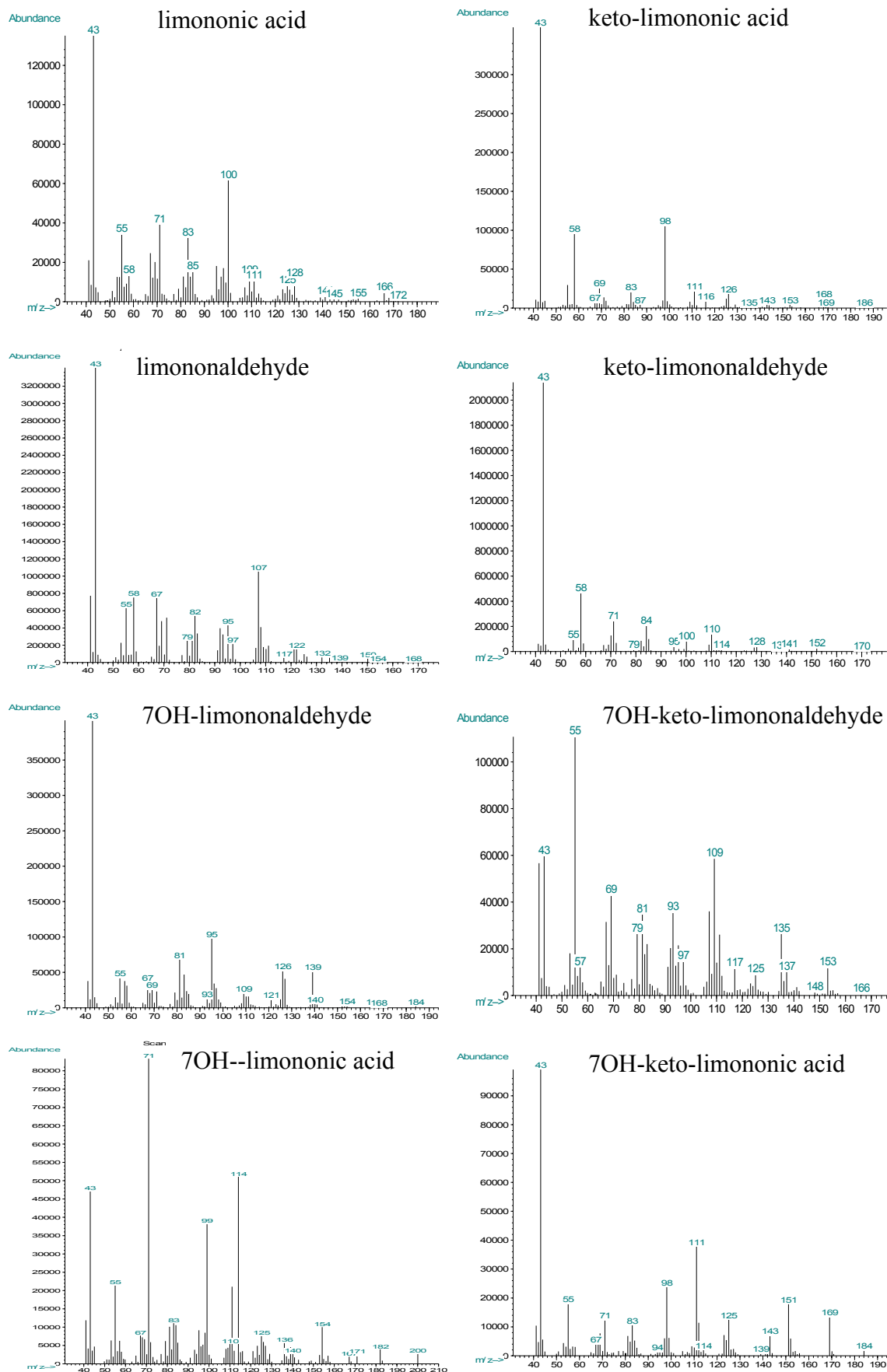


Figure 2. Mass spectrum of particle phase products from d-limonene and ozone reactions.

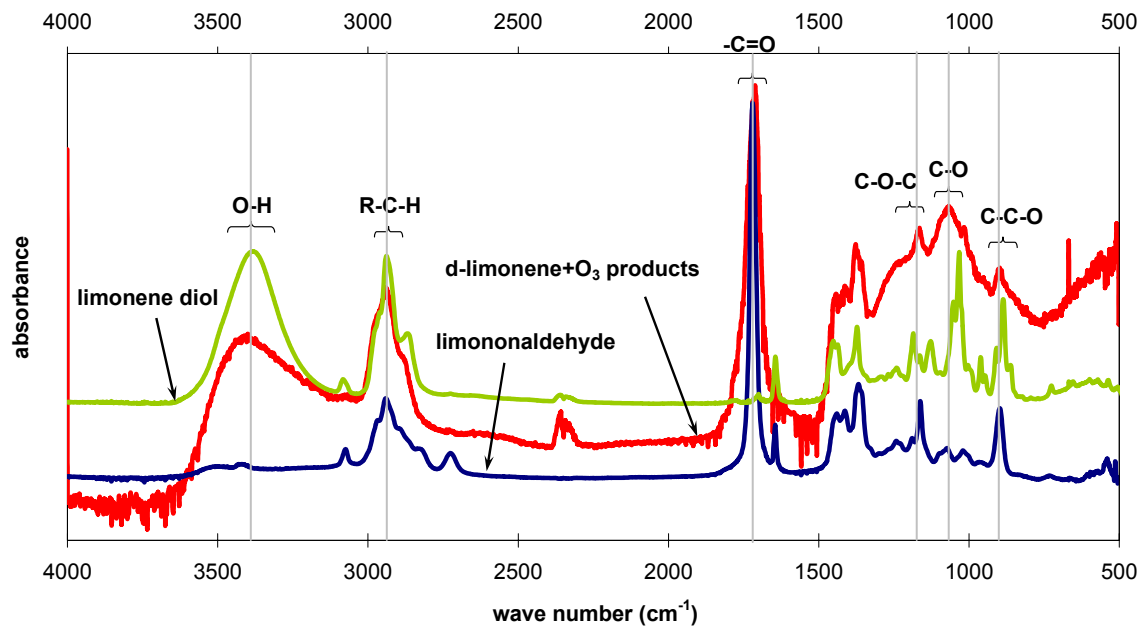
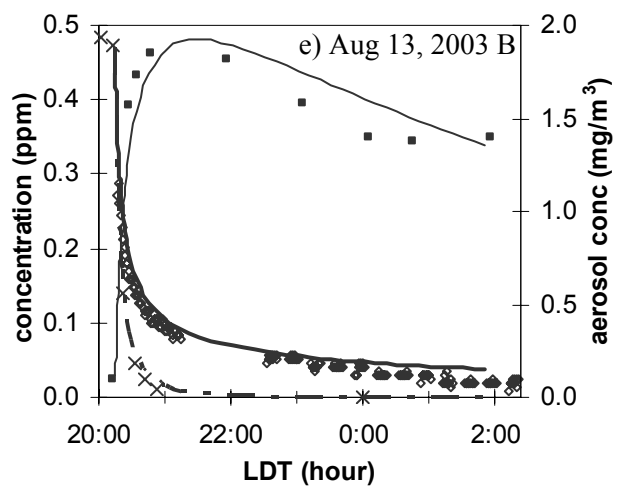
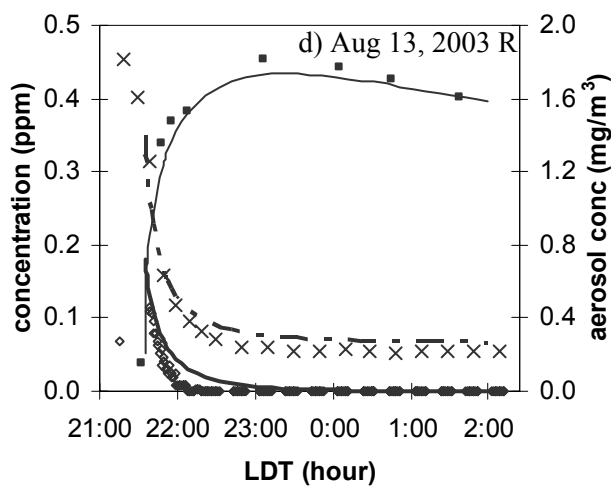
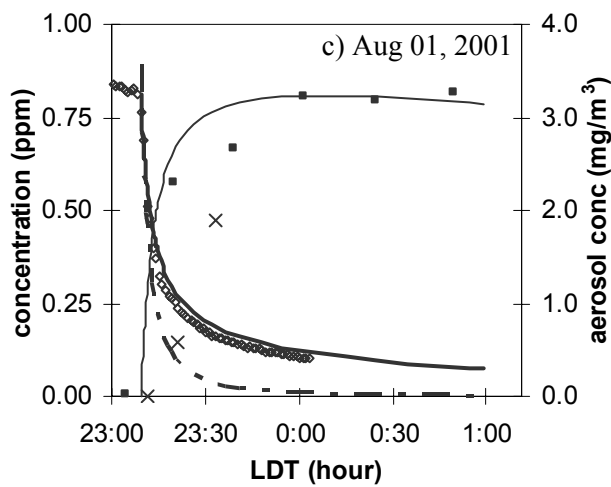
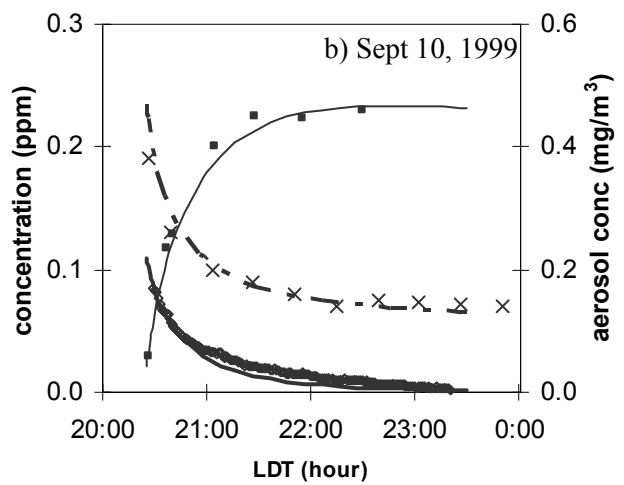
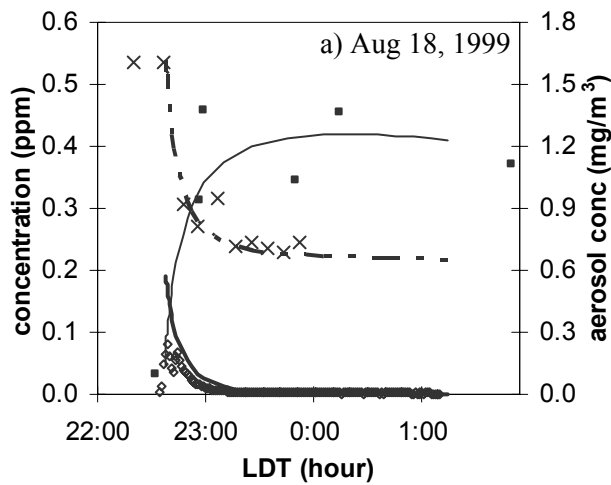


Figure 3. FTIR spectra of d-limonene reaction products with ozone comparing with those of limonene diol and limononaldehyde standards.



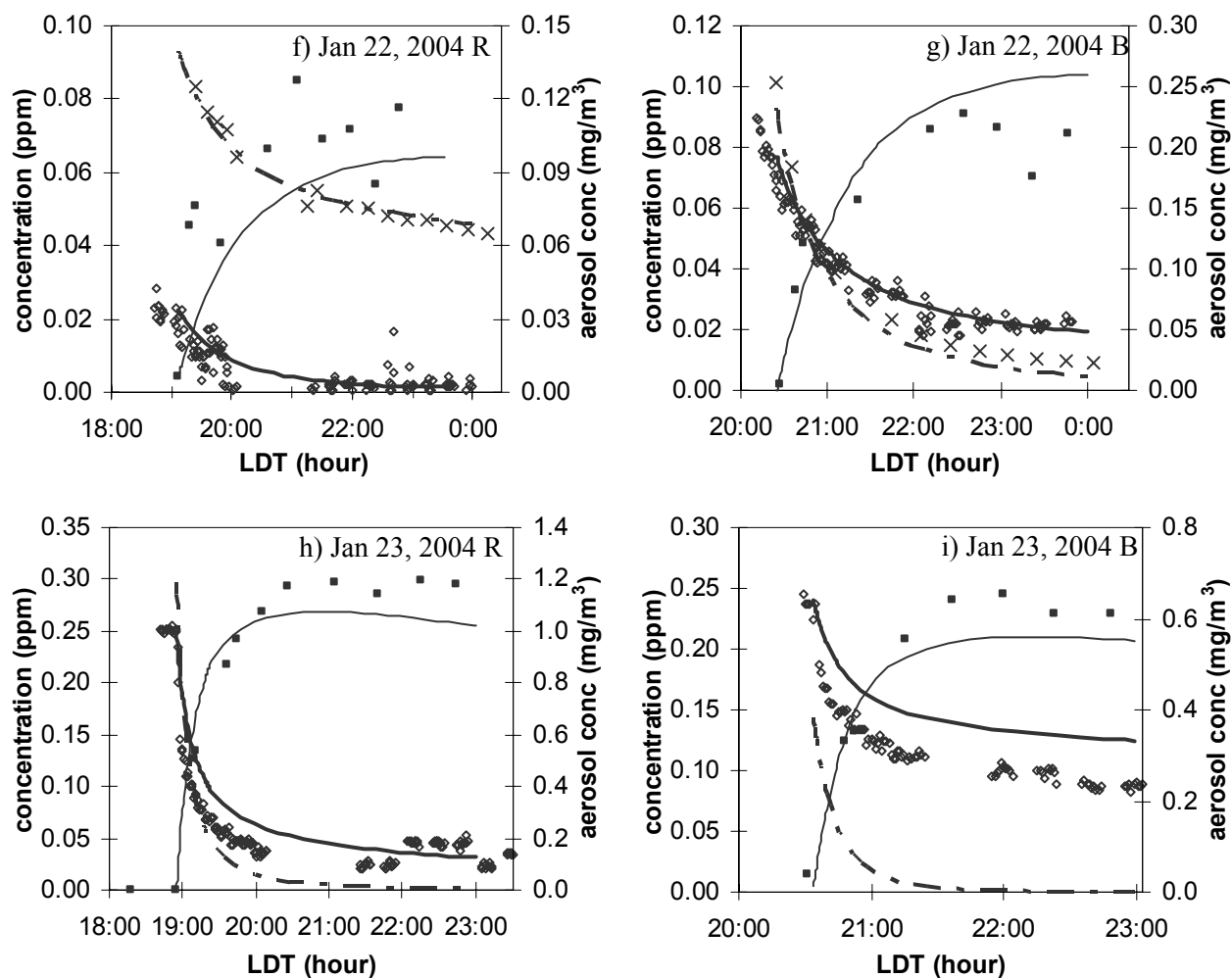
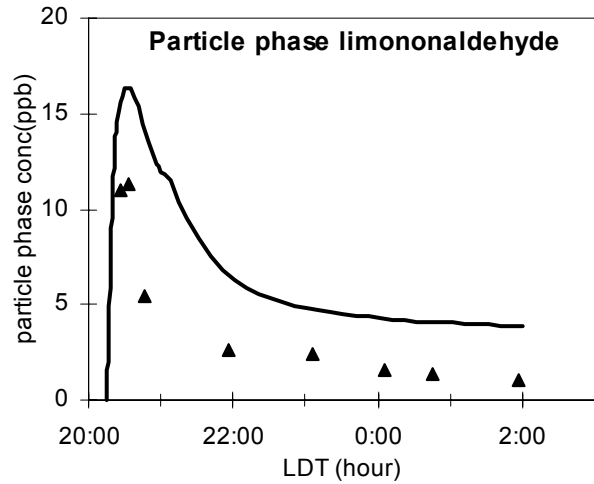
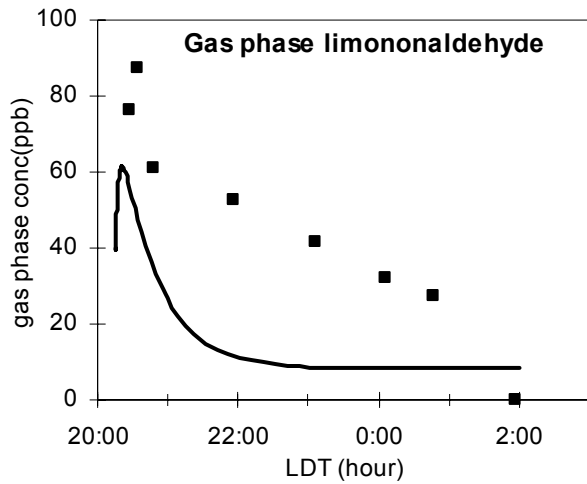


Figure 4. Model simulations (lines) vs experimental data (symbols) for d-limonene with ozone experiments. LDT is local daylight-saving time. Thick line (—) is simulated ozone, dash line (- · -) is simulated d-limonene, line (—) is simulated aerosol, diamond (◇) is measured ozone, cross mark (×) is measured d-limonene, solid square (■) is measured aerosol.

a) limononaldehyde



b) keto-limononaldehyde

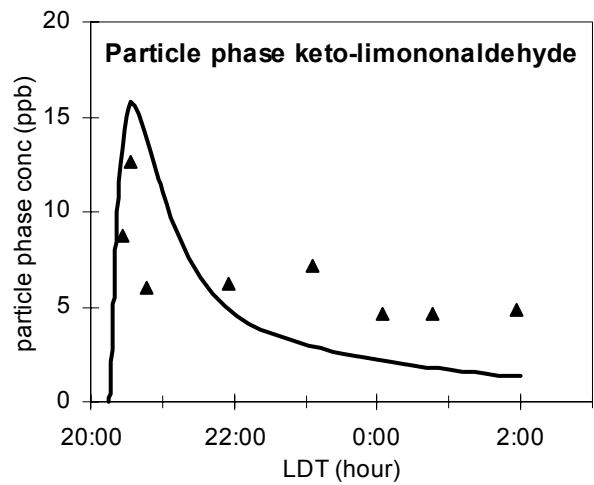
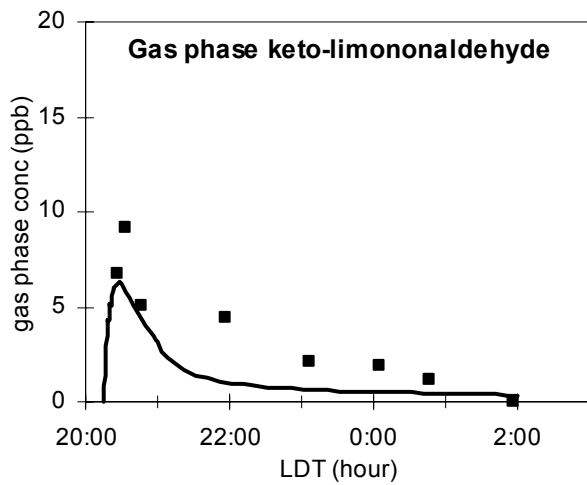
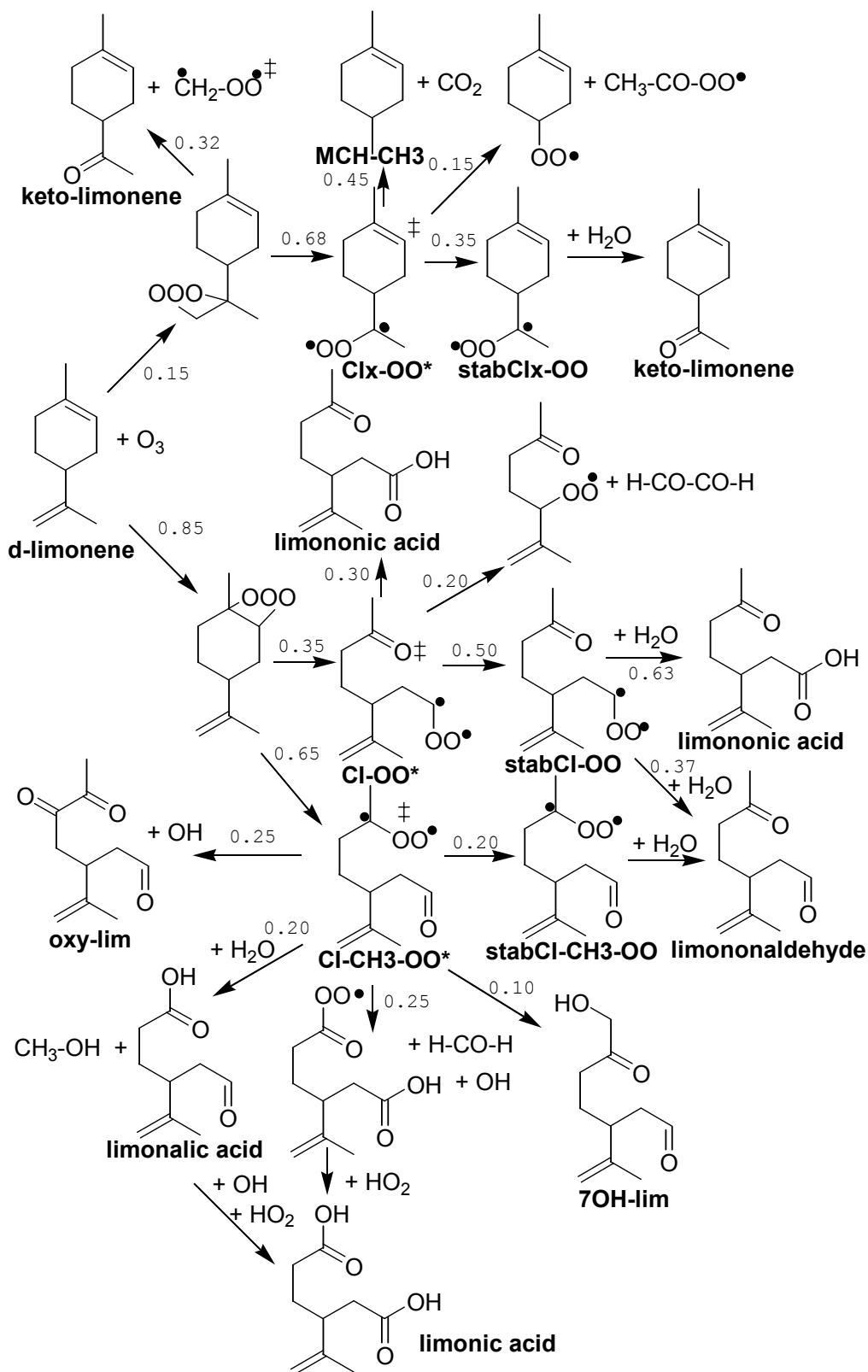


Figure 5. Simulations (lines) vs data (symbols) of (a) limononaldehyde and (b) keto-limononaldehyde in gas and particle phases from Aug 13, 2003 B experiment.



Scheme I. d-limonene + O_3 reaction pathway for model products and product yields.

	Rxn. ID.		rate	Reference
		d-limonene gas phase reactions	sec ⁻¹ or cm ³ molecule ⁻¹ sec ⁻¹	
1	LOH1	limonene+OH→0.37×lim-OH-xOO+0.63×lim-OH-iOO	4.2E-11×EXP(401/TK)	1, 2
2	LH1	lim-OH-iOO+HO2→lim-OH-iOOH+O2	2.9E-13×EXP(1250/TK)	3
3	LH2	lim-OH-xOO+HO2→0.8×(lim-OH-xOOH+O2)+ 0.2×(lim-OH=xO+H2O+O2)	2.9E-13×EXP(1250/TK)	3
4	LO3P_1	limonene+O3P→0.65×limonene-oxide+0.35×(1.1×keto-limonene)	71.9E-12	1, 4
5	LO3	limonene+O3→0.85×(0.65×CI-CH3-OO*+0.35×CI-OO*)+ 0.15×(0.68×(CIx-OO*+H-CO-H)+0.32×(keto-limonene+[.CH2OO.]*))	2.65e-15×EXP(-783/TK)	5, 6
6	LS1	lim-OH-iOO+RO2→0.6×(limononaldehyde+H2O2)+ 0.2×(limononaldehyde+limononic_acid)	1.4e-12	3
7	LS2	lim-OH-xOO+RO2→0.9×(keto-limonene+H-CO-H+H2O2)+ 0.1×(MCH=O+CH3-CO-CH2-OH+HO2+XHO2)	1.2E-12	3
8	LS3	lim-CO-OO+RO2→0.7×(norlim-OO+CO2)+0.3×(limononic_acid+XHO2)	1.7E-11	3
9	LS4	norlim-OO+RO2→0.8×(norlim+HO2)+0.2×(norlim-OH+XHO2)	1.2E-12	3
10	LS5	ketolim-CO-OO+RO2→0.7×(nor-ketolim-OO+O2)+ 0.3×(keto-limononic_acid+O2+XHO2)	1.7E-11	3
11	LS6	MCH-OO+RO2→0.8×(MCH=O+HO2+O2)+0.2×(MCH-OH+XHO2)	1.4e-12	3
12	LS7	limonic_acid-CO-OO+RO2→0.3×(limonic_acid+XHO2)+0.7×(oxy-C=C7)	1.7E-11	3
13	LS8	CH3-CO-OO.+RO2→0.7×(CH3-OO.+CO2)+0.3×(CH3-CO-OH+XHO2)	5.1E-12×EXP(272/TK)	
14	LS9	XOH-OOH-lim-CO-OO+RO2→0.7×(XOH-OOH-norlim+CO2+HO2+XO2)+ 0.3×(XOH-OOH-lim-CO-OH+XHO2)	1.7E-11	3
15	LS10	ketolim-OH-iOO+RO2→0.6×(ketolim+HO2)+ 0.2×(ketolim+keto-limononic_acid)	1.4e-12	3
16	LS12	nor-ketolim-OO+RO2→0.8×(nor-ketolim+HO2)+ 0.2×(nor-ketolim-OH+XHO2)	4.4E-14	3
17	LS13	C=C7-OO+RO2→0.6×(C=C7+HO2)+0.2×(C=C7+XHO2)+ 0.2×(CH2=C(CH3)-CO-H+C4+XO2+HO2+XHO2)	3.0E-17	3
18	LS14	norlim-CO-OO+RO2→0.7×(C=C7-OO+CO2+O2)+ 0.3×(norlimononic_acid+XHO2)	1.7E-11	3
19	LS15	nor-ketolim-CO-OO+RO2→0.7×(C7-OO+CO2+O2)+ 0.3×(keto-norlimononic_acid+XHO2)	1.7E-11	3
20	LS18	CH3-CO-CH2-OO+RO2→0.8×(CH3-CO-CO-H+HO2)+ 0.2×(CH3-CO-CH2-OH+XHO2)	2.7E-12	3
21	LS19	C7-OO+RO2→CH3-CO-CO-H+CH3-CO-CH2-CO-H+XO2+HO2	4.4E-14	3
22	LS20	CH3-OO.+RO2→H-CO-H+HO2+O2	1.1E-13×EXP(365/TK)	1
23	LS21	HO-CH2-OO.+RO2→0.8×(H-CO-OH+O2)+0.2×(HO-CH2-OH+XHO2)	2.7E-12	3
24	LS22	HO-CH2-CO-OO.+RO2→0.7×(HO-CH2-OO.+CO2+O2)+ 0.3×(HO-CH2-CO-OH+XHO2)	1.7E-11	3
25	LS23	HO-CH2-CH2-OO.+RO2→0.8×(HO-CH2-CO-H+HO2)+ 0.2×(HO-CH2-CH2-OH+XHO2)	2.7E-12	3

26	LS24	$H-CO-CO-OO.+RO_2 \rightarrow 0.7 \times (CO+HO_2+CO_2+O_2)+0.3 \times (H-CO-CO-OH+XHO_2)$	1.7E-11	3
27	LS25	$7OH-lim-CO-OO+RO_2 \rightarrow 0.7 \times (7OH-norlim+XO_2+HO_2+CO_2+O_2)+0.3 \times (7OH-lim-CO-OH+XHO_2)$	1.7E-11	3
28	LOO_xO2_1	$lim-OH-iOO+XO_2 \rightarrow limononaldehyde+HO_2$	$3.8e-13 \times EXP(800/TK)$	
29	LOO_xO2_2	$lim-OH-xOO+XO_2 \rightarrow keto-limonene+H-CO-H+HO_2$	$3.8e-13 \times EXP(800/TK)$	
30	LOO_xO2_3	$CH_3-CO-OO.+XO_2 \rightarrow CH_3-OO.+CO_2$	$1.0e-12 \times EXP(800/TK)$	
31	LOO_xO2_4	$lim-CO-OO+XO_2 \rightarrow norlim-OO+CO_2$	$1.0e-12 \times EXP(800/TK)$	
32	LOO_xO2_5	$ketolim-CO-OO+XO_2 \rightarrow nor-ketolim+HO_2+CO_2+XO_2$	$1.0e-12 \times EXP(800/TK)$	
33	LOO_xO2_6	$MCH-OO+XO_2 \rightarrow MCH=O+HO_2$	$3.8e-13 \times EXP(800/TK)$	
34	LOO_xO2_7	$XOH-OOH-lim-CO-OO+XO_2 \rightarrow XOH-OOH-norlim+HO_2+CO_2+XO_2$	$1.0e-12 \times EXP(800/TK)$	
35	LOO_xO2_8	$ketolim-OH-iOO+XO_2 \rightarrow ketolim+HO_2$	$3.8e-13 \times EXP(800/TK)$	
36	LOO_xO2_9	$norlim-OO+XO_2 \rightarrow norlim+HO_2$	$3.8e-13 \times EXP(800/TK)$	
37	LOO_xO2_10	$nor-ketolim-OO+XO_2 \rightarrow nor-ketolim+HO_2$	$3.8e-13 \times EXP(800/TK)$	
38	LOO_xO2_11	$C=C_7-OO+XO_2 \rightarrow C=C_7+HO_2$	$3.8e-13 \times EXP(800/TK)$	
39	LOO_xO2_12	$norlim-CO-OO+XO_2 \rightarrow C=C_7-OO+CO_2$	$1.0e-12 \times EXP(800/TK)$	
40	LOO_xO2_13	$nor-ketolim-CO-OO+XO_2 \rightarrow C_7+HO_2+CO_2+XO_2$	$1.0e-12 \times EXP(800/TK)$	
41	LOO_xO2_16	$CH_3-CO-CH_2-OO+XO_2 \rightarrow CH_3-CO-OO.+H-CO-H$	$3.8e-13 \times EXP(800/TK)$	
42	LOO_xO2_17	$C_7-OO+XO_2 \rightarrow C_7+HO_2$	$3.8e-13 \times EXP(800/TK)$	
43	LOO_xO2_18	$CH_3-OO.+XO_2 \rightarrow H-CO-H+HO_2$	$3.8e-13 \times EXP(800/TK)$	
44	LOO_xO2_19	$HO-CH_2-OO.+XO_2 \rightarrow H-CO-OH+HO_2$	$3.8e-13 \times EXP(800/TK)$	
45	LOO_xO2_20	$HO-CH_2-CO-OO.+XO_2 \rightarrow H-CO-H+CO_2+HO_2$	$1.0e-12 \times EXP(800/TK)$	
46	LOO_xO2_21	$HO-CH_2-CH_2-OO.+XO_2 \rightarrow HO-CH_2-CH_2-O.$	$3.8e-13 \times EXP(800/TK)$	
47	LOO_xO2_22	$H-CO-CO-OO.+XO_2 \rightarrow HO_2+CO+CO_2$	$1.0e-12 \times EXP(800/TK)$	
48	LOO_xO2_23	$7OH-lim-CO-OO+XO_2 \rightarrow 7OH-norlim+CO_2+XO_2+HO_2$	$1.0e-12 \times EXP(800/TK)$	
49	LOO_xO2_24	$limonic_acid-CO-OO+XO_2 \rightarrow oxy-C=C_7+XO_2+HO_2+CO_2$	$1.0e-12 \times EXP(800/TK)$	
50	LOO_xO2_25	$XOH-ONO_2-lim-CO-OO+XO_2 \rightarrow XOH-ONO_2-norlim+XO_2+HO_2+CO_2$	$1.0e-12 \times EXP(800/TK)$	
51	XHO2	$XHO_2+HO_2 \rightarrow$	$2.9E-13 \times EXP(1250/TK)$	
		Criegee Reactions		
52	CI1	$CI-CH_3-OO^* \rightarrow 0.2 \times (limonic_acid+CH_3-OH)+0.2 \times stabCI-CH_3-OO+0.1 \times (7OH-lim)+0.50 \times (0.5 \times (oxy-lim+XO_2+HO_2)+0.5 \times (limonic_acid-CO-OO+H-CO-H))+0.89 \times OH+0.01 \times O_3P$	1e6	7
53	CI1a	$limonic_acid-CO-OO+HO_2 \rightarrow 0.3 \times (limonic_acid+O_3)+0.7 \times (limonic_acid-CO-OOH+O_2)$	$2.9E-13 \times EXP(1250/TK)$	3
54	CI1_1add	$lim-7O. \rightarrow 0.80 \times (0.8 \times limonic_acid+0.2 \times (2(CHO-CH_2)-CH-(CH_3-C=CH_2)+CO_2)+H-CO-H)+0.20 \times (0.8 \times 7OH-lim-CO-OH+0.2 \times (norlim+CO_2))$	1e4	
55	Lp101	$7OH-lim-CO-OO+HO_2 \rightarrow 0.4 \times (7OH-lim-CO-OOH+O_2)+0.6 \times (7OH-lim-CO-OH+O_3)$	$2.9E-13 \times EXP(1250/TK)$	3
56	CI2	$CI-OO^* \rightarrow 0.2 \times (C=C_7-OO+H-CO-CO-H+XO_2)+0.3 \times limononic_acid+0.5 \times stabCI-OO+0.89 \times OH+0.01 \times O_3P$	1e6	7
57	CI3	$CIx-OO^* \rightarrow 0.15 \times (MCH-OO+CH_3-CO-OO.)+0.45 \times (MCH-CH_3+CO_2)+$	1e6	7

		$0.35 \times \text{stabCIx-OO} + 0.05 \times (\text{keto-limonene}) + 0.89 \times \text{OH} + 0.01 \times \text{O3P}$		
58	CI2_k	$\text{ketoCI-OO}^* \rightarrow 0.2 \times (\text{C7+H-CO-CO-H} + 2 \times \text{XO2}) + 0.3 \times \text{keto-limononic_acid} + 0.5 \times \text{stab_ketoCI-OO} + 0.89 \times \text{OH} + 0.01 \times \text{O3P}$	1e6	7
59	CI1_k	$\text{ketoCI-CH3-OO}^* \rightarrow 0.25 \times (\text{C6-CHO} + \text{CH3-CO-OO} + \text{XO2}) + 0.35 \times \text{stab_ketoCI-CH3-OO} + 0.05 \times (\text{ketolim}) + 0.35 \times (\text{C7-CHO} + \text{CO2}) + 0.89 \times \text{OH} + 0.01 \times \text{O3P}$	1e6	7
60	CI3_k	$\text{limCIx-OO}^* \rightarrow 0.15 \times (\text{C6-CHO} + \text{CH3-CO-OO} + \text{XO2}) + 0.45 \times (1.167 \times \text{C6-CHO} + \text{CO2}) + 0.35 \times \text{stab_limCIx-OO} + 0.05 \times (\text{ketolim} + \text{H-CO-H}) + 0.89 \times \text{OH} + 0.01 \times \text{O3P}$	1e6	7
61	stab2	$\text{stabCI-OO} + \text{H2O} \rightarrow 0.625 \times (\text{limononic_acid} + \text{H2O}) + 0.375 \times (\text{limononaldehyde} + \text{H2O2})$	1.6E-17	3, 8
62	stab8	$\text{stabCI-OO} + \text{CO} \rightarrow \text{limononaldehyde} + \text{CO2}$	1.2E-15	
63	stab10	$\text{stabCI-OO} + \text{limononaldehyde} \rightarrow \text{seed}$	2E-14	9
64	stab12	$\text{stabCI-OO} + \text{ketolim} \rightarrow \text{seed}$	2E-14	9
65	stab13	$\text{stabCI-OO} + \text{H-CO-OH} \rightarrow \text{seed}$	2E-14	9
66	stab14	$\text{stabCI-OO} + \text{H-CO-H} \rightarrow \text{limononic_acid} + \text{H-CO-H}$	4E-16	10
67	stab14_1	$\text{stabCI-OO} + 7\text{OH-lim} \rightarrow \text{seed}$	2E-14	9
68	stab14_2	$\text{stabCI-OO} + \text{C6-CHO} \rightarrow \text{seed}$	2E-14	9
69	stab14_3	$\text{stabCI-OO} + \text{keto-limononic_acid} \rightarrow \text{seed}$	5.3E-13	
70	stab14_4	$\text{stabCI-OO} + \text{limononic_acid} \rightarrow \text{seed}$	5.3E-13	
71	stab15	$\text{stabCI-CH3-OO} + \text{H2O} \rightarrow \text{limononaldehyde} + \text{H2O2}$	6E-18	
72	stab18	$\text{stabCI-CH3-OO} + \text{CO} \rightarrow \text{limononaldehyde} + \text{CO2}$	1.2E-15	
73	stab19	$\text{stabCI-CH3-OO} + \text{limononaldehyde} \rightarrow \text{seed}$	2E-14	9
74	stab20	$\text{stabCI-CH3-OO} + \text{ketolim} \rightarrow \text{seed}$	2E-14	9
75	stab21	$\text{stabCI-CH3-OO} + \text{H-CO-OH} \rightarrow \text{seed}$	2E-14	9
76	stab22	$\text{stabCI-CH3-OO} + \text{H-CO-H} \rightarrow \text{limononic_acid} + \text{H-CO-H}$	4E-16	10
77	stab22_1	$\text{stabCI-CH3-OO} + 7\text{OH-lim} \rightarrow \text{seed}$	2E-14	9
78	stab22_2	$\text{stabCI-CH3-OO} + \text{C6-CHO} \rightarrow \text{seed}$	2E-14	9
79	stab22_3	$\text{stabCI-CH3-OO} + \text{keto-limononic_acid} \rightarrow \text{seed}$	5.3E-13	
80	stab22_4	$\text{stabCI-CH3-OO} + \text{limononic_acid} \rightarrow \text{seed}$	5.3E-13	
81	stab23	$\text{stab_ketoCI-OO} + \text{H2O} \rightarrow 0.625 \times (\text{keto-limononic_acid} + \text{H2O}) + 0.375 \times (\text{ketolim} + \text{H2O2})$	1.6E-17	
82	stab26	$\text{stab_ketoCI-OO} + \text{CO} \rightarrow \text{ketolim} + \text{CO2}$	1.2E-15	
83	stab27	$\text{stab_ketoCI-OO} + \text{limononaldehyde} \rightarrow \text{seed}$	2E-14	9
84	stab28	$\text{stab_ketoCI-OO} + \text{ketolim} \rightarrow \text{seed}$	2E-14	9
85	stab29	$\text{stab_ketoCI-OO} + \text{H-CO-OH} \rightarrow \text{seed}$	2E-14	9
86	stab30	$\text{stab_ketoCI-OO} + \text{H-CO-H} \rightarrow \text{keto-limononic_acid} + \text{H-CO-H}$	4E-16	10
87	stab30_1	$\text{stab_ketoCI-OO} + 7\text{OH-lim} \rightarrow \text{seed}$	2E-14	9
88	stab30_2	$\text{stab_ketoCI-OO} + \text{C6-CHO} \rightarrow \text{seed}$	2E-14	9
89	stab30_3	$\text{stab_ketoCI-OO} + \text{keto-limononic_acid} \rightarrow \text{seed}$	2E-14	9
90	stab30_4	$\text{stab_ketoCI-OO} + \text{limononic_acid} \rightarrow \text{seed}$	5.3E-13	

91	stab31	stab_ketoCI-CH3-OO+H2O→ketolim+H2O2	6E-18	
92	stab34	stab_ketoCI-CH3-OO+CO→ketolim+CO2	1.2E-15	
93	stab35	stab_ketoCI-CH3-OO+limononaldehyde→seed	2E-14	9
94	stab36	stab_ketoCI-CH3-OO+ketolim→seed	2E-14	9
95	stab37	stab_ketoCI-CH3-OO+H-CO-OH→seed	2E-14	9
96	stab38	stab_ketoCI-CH3-OO+H-CO-H→limononic_acid+H-CO-H	4E-16	10
97	stab38_1	stab_ketoCI-CH3-OO+7OH-lim→seed	2E-14	9
98	stab38_2	stab_ketoCI-CH3-OO+C6-CHO→seed	2E-14	9
99	stab38_3	stab_ketoCI-CH3-OO+keto-limononic_acid→seed	5.3E-13	
100	stab38_4	stab_ketoCI-CH3-OO+limononic_acid→seed	5.3E-13	
101	stab39	stabCIx-OO+H2O→0.625×(acid_limonene+H2O)+ 0.375×(keto-limonene+H2O2)	6E-18	
102	stab42	stabCIx-OO+CO→keto-limonene+CO2	1.2E-15	
103	stab43	stabCIx-OO+limononaldehyde→seed	2E-14	9
104	stab44	stabCIx-OO+ketolim→seed	2E-14	9
105	stab45	stabCIx-OO+H-CO-OH→seed	2E-14	9
106	stab46	stabCIx-OO+H-CO-H→acid_limonene+H-CO-H	4E-16	10
107	stab46_1	stabCIx-OO+7OH-lim→seed	2E-14	9
108	stab46_2	stabCIx-OO+C6-CHO→seed	2E-14	9
109	stab46_3	stabCIx-OO+keto-limononic_acid→seed	5.3E-13	
110	stab46_4	stabCIx-OO+limononic_acid→seed	5.3E-13	
111	stab47	stab_limCIx-OO+H2O→ 0.625×(acid_lim+H2O)+ 0.375×(oxo_lim+H2O2)	6E-18	
112	stab50	stab_limCIx-OO+CO→oxo_lim+CO2	1.2E-15	
113	stab51	stab_limCIx-OO+limononaldehyde→seed	2E-14	9
114	stab52	stab_limCIx-OO+ketolim→seed	2E-14	9
115	stab53	stab_limCIx-OO+H-CO-OH→seed	2E-14	9
116	stab54	stab_limCIx-OO+H-CO-H→acid_lim+H-CO-H	4E-16	10
117	stab54_1	stab_limCIx-OO+7OH-lim→seed	2E-14	9
118	stab54_2	stab_limCIx-OO+C6-CHO→seed	2E-14	9
119	stab54_3	stab_limCIx-OO+keto-limononic_acid→seed	5.3E-13	
120	stab54_4	stab_limCIx-OO+limononic_acid→seed	5.3E-13	
121	stab55	stab_MCHCI-OO+H2O→0.625×(C6-CO-OH+H2O)+ 0.375×(C6-CHO+ H2O2)	1.6E-17	
122	stab58	stab_MCHCI-OO+CO→C6-CHO+CO2	1.2E-15	
123	stab59	stab_MCHCI-OO+limononaldehyde→seed	2E-14	9
124	stab60	stab_MCHCI-OO+ketolim→seed	2E-14	9
125	stab61	stab_MCHCI-OO+H-CO-OH→seed	2E-14	9
126	stab62	stab_MCHCI-OO+H-CO-H→C6-CO-OH+H-CO-H	4E-16	10
127	stab62_1	stab_MCHCI-OO+7OH-lim→seed	2E-14	9
128	stab62_2	stab_MCHCI-OO+C6-CHO→seed	2E-14	9

129	stab62_3	stab_MCHCI-OO+keto-limononic_acid→seed	5.3E-13	
130	stab62_4	stab_MCHCI-OO+limononic_acid→seed	5.3E-13	
131	stab63	stab_MCHCI-CH3-OO+H2O→C6-CHO+H2O2	6E-18	
132	stab66	stab_MCHCI-CH3-OO+CO→C6-CHO+CO2	1.2E-15	
133	stab67	stab_MCHCI-CH3-OO+limononaldehyde→seed	2E-14	9
134	stab68	stab_MCHCI-CH3-OO+ketolim→seed	2E-14	9
135	stab69	stab_MCHCI-CH3-OO+H-CO-OH→seed	2E-14	9
136	stab70	stab_MCHCI-CH3-OO+H-CO-H→C6-CO-OH+H-CO-H	4E-16	10
137	stab70_1	stab_MCHCI-CH3-OO+7OH-lim→seed	2E-14	9
138	stab70_2	stab_MCHCI-CH3-OO+C6-CHO→seed	2E-14	9
139	stab70_3	stab_MCHCI-CH3-OO+keto-limononic_acid→seed	5.3E-13	
140	stab70_4	stab_MCHCI-CH3-OO+limononic_acid→seed	5.3E-13	
		Gas phase product reactions		
141	Lp4	limononaldehyde+OH→0.3×(lim-CO-OO+H2O)+ 0.7×(0.8×(ketolim+XO2+H-CO-H)+0.2×(oxo_acid)+0.6×HO2)	11e-11	
142	Lp3	limononaldehyde→norlim-OO+HO2+CO	j[[pinald_to_prods]	
143	LO3P_2	limononaldehyde+O3P→1.1×ketolim	3.63e-11	
144	Lp6	limononaldehyde+O3→0.68×(limCIx-OO*+H-CO-H)+ 0.32×(ketolim+[.CH2OO.]*)+0.89×OH	8.3E-18	
145	Lp7	lim-CO-OO+HO2→0.3×(limononic_acid+O3)+0.7×(lim-CO-OOH+O2)	2.9E-13×EXP(1250/TK)	3
146	LH5	norlim-OO+HO2→0.7×(norlim-OOH+O2)+0.3×(norlim+H2O+O2)	2.9E-13×EXP(1250/TK)	3
147	Lp30	keto-limonene+OH→ketolim-OH-iOO	7.15e-11	2
148	LO3P_3	keto-limonene+O3P→ketolim	4.67E-11	
149	Lp32	keto-limonene+O3→0.65×ketoCI-CH3-OO*+0.35×ketoCI-OO*+ 0.86×OH	1.8e-16	
150	Lp30b	ketolim-OH-iOO+HO2→ketolim-OH-iOOH	2.86E-13×EXP(1250/TK)	3
151	Lp27d	lim-OH=xO+OH→0.95×(lim-XO-OH+XO2+HO2)+ 0.05×(keto-limonene+H2O+CO+HO2)	11e-11	
152	Lp26b	lim-OH-xOOH+OH→0.88×(0.8×(lim-XOH-OOH+XO2+HO2)+ 0.2×(oxo_acid))+0.12×(keto-limonene+0.35×OH+ 0.65×XO2+H-CO-H+ HO2+0.65×H2O)	11e-11	
153	Lp32_d	lim-OH-xOOH+O3→0.65×(ketoCI-CH3-OO*+H-CO-H+H2O)+ 0.35×(ketoCI-OO*+H-CO-H+H2O)+0.86×OH	1.8e-16	
154	Lp52a	acid_limonene+OH→1.1×keto-limononic_acid+XO2+HO2	11e-11	
155	Lp52b	acid_limonene+O3→0.65×(1.1×keto-limononic_acid)+ 0.35×(1.25×keto-limononic_acid)+0.86×OH	1.8e-16	
156	Lp29b	limonene-oxide+OH→1.0×(keto-limonene-oxide+H-CO-H+XO2+HO2)	11e-11	2
157	Lp29c	limonene-oxide+O3→keto-limonene-oxide+[.CH2OO.]*+0.86×OH	8.3E-18	
158	Lp29x	limonene-oxide+O3P→keto-limonene-oxide+H-CO-H+XO2	2.5E-11	
159	Lp22	limononic_acid+OH→0.05×(0.8×(H-CO-CO-OH+C=C7+XO2)+ 0.2×(C6-CO-OH+CH3-CO-CH2-OH+XO2+HO2)+XO2)+	8.25e-11	

		$0.95 \times (\text{keto-limononic_acid} + \text{HO}_2 + \text{H-CO-H} + \text{XO}_2)$		
160	LO3P_4	$\text{limononic_acid} + \text{O}_3 \rightarrow \text{keto-limononic_acid}$	2.5E-11	
161	Lp21	$\text{limononic_acid} + \text{O}_3 \rightarrow \text{keto-limononic_acid} + 0.2 \times [\text{.CH}_2\text{OO.}]^* + 0.8 \times \text{H-CO-H} + 0.86 \times \text{OH}$	8.3E-18	
162	Lp56	$\text{limononic_acid} + \text{OH} \rightarrow 0.3 \times (\text{limononic_acid-CO-OO} + \text{HO}_2) + 0.7 \times (\text{keto-limononic_acid} + \text{HO}_2 + \text{H-CO-H} + \text{XO}_2)$	78.9E-12	2
163	Lp56a	$\text{limononic_acid} + \text{O}_3 \rightarrow \text{keto-limononic_acid} + 0.2 \times [\text{.CH}_2\text{OO.}]^* + 0.8 \times \text{H-CO-H} + 0.86 \times \text{OH}$	8.3E-18	
164	Lp51a	$\text{limononic_acid-CO-OOH} + \text{OH} \rightarrow 0.05 \times (\text{norlim-CO-OO} + \text{H}_2\text{O}) + 0.95 \times (\text{nor-ketolim-CO-OOH} + \text{HO}_2 + \text{H-CO-H} + \text{XO}_2)$	11e-11	
165	Lp51b	$\text{limononic_acid-CO-OOH} + \text{O}_3 \rightarrow \text{nor-ketolim-CO-OOH} + 0.2 \times [\text{.CH}_2\text{OO.}]^* + 0.8 \times \text{H-CO-H} + 0.86 \times \text{OH}$	8.3E-18	
166	LY1_10	$\text{limononic_acid} + \text{OH} \rightarrow \text{keto-limononic_acid} + \text{H-CO-H} + \text{XO}_2 + \text{HO}_2$	11e-11	
167	LY1_10a	$\text{limononic_acid} + \text{O}_3 \rightarrow \text{keto-limononic_acid} + 0.2 \times [\text{.CH}_2\text{OO.}]^* + 0.8 \times \text{H-CO-H} + 0.86 \times \text{OH}$	8.3E-18	
168	Lp24b	$\text{norlimononic_acid} + \text{OH} \rightarrow \text{keto-norlimononic_acid} + \text{HO}_2 + \text{H-CO-H} + \text{XO}_2$	11e-11	
169	Lp24c	$\text{norlimononic_acid} + \text{O}_3 \rightarrow \text{keto-norlimononic_acid} + 0.2 \times [\text{.CH}_2\text{OO.}]^* + 0.8 \times \text{H-CO-H} + 0.86 \times \text{OH}$	8.3E-18	
170	Lp27d2	$\text{lim-OH=iO} + \text{OH} \rightarrow 0.9 \times (0.35 \times (\text{ketolim-OH=iO} + \text{H-CO-H} + \text{HO}_2) + 0.65 \times \text{CH}_3\text{-CO-CH}_2\text{-OH} + \text{C}_7\text{-OO}) + 0.1 \times (\text{limononaldehyde} + 2 \times \text{XO}_2 + \text{HO}_2)$	59.257e-12	2
171	Lp27d3	$\text{lim-OH=iO} + \text{O}_3 \rightarrow \text{ketolim-OH=iO} + 0.2 \times [\text{.CH}_2\text{OO.}]^* + 0.8 \times \text{H-CO-H} + 0.86 \times \text{OH}$	8.3E-18	
172	Lp27b	$\text{lim-OH-iOOH} + \text{OH} \rightarrow 0.66 \times (\text{ketolim-OH-iOOH} + \text{H-CO-H} + \text{XO}_2 + \text{HO}_2) + 0.14 \times (\text{limononic_acid} + \text{HO}_2 + \text{H}_2\text{O}) + 0.13 \times (\text{lim-OH-iOO} + \text{H}_2\text{O}) + 0.07 \times (\text{limononaldehyde} + \text{OH} + \text{HO}_2)$	7.44E-11	
173	Lp32_c	$\text{lim-OH-iOOH} + \text{O}_3 \rightarrow 0.84 \times (\text{CIx-OO}^* + \text{H-CO-H} + \text{H}_2\text{O}) + 0.16 \times (\text{ketolim} + [\text{.CH}_2\text{OO.}]^* + \text{H}_2\text{O}) + 0.86 \times \text{OH}$	8.3E-18	
174	Lp7_a	$\text{lim-CO-OOH} + \text{OH} \rightarrow 0.05 \times (\text{lim-CO-OO} + \text{H}_2\text{O}) + 0.95 \times (\text{ketolim-CO-OOH} + \text{H-CO-H} + \text{HO}_2 + \text{XO}_2)$	5.9E-11	
175	Lp7_a1	$\text{lim-CO-OOH} + \text{O}_3 \rightarrow \text{ketolim-CO-OOH} + 0.2 \times [\text{.CH}_2\text{OO.}]^* + 0.8 \times \text{H-CO-H} + 0.86 \times \text{OH}$	8.3E-18	
176	Lp105	$7\text{OH-lim} + \text{OH} \rightarrow 0.7 \times (7\text{OH-ketolim} + \text{XO}_2 + \text{H-CO-H} + \text{HO}_2) + 0.3 \times (7\text{OH-lim-CO-OO} + \text{H}_2\text{O})$	5.9E-11	
177	Lp106	$7\text{OH-lim} + \text{O}_3 \rightarrow 0.84 \times (\text{limCIx-OO}^* + \text{H-CO-H}) + 0.16 \times (7\text{OH-ketolim} + [\text{.CH}_2\text{OO.}]^*)$	8.3E-18	
178	Lp109	$7\text{OH-lim-CO-OH} + \text{OH} \rightarrow 7\text{OH-ketolim-CO-OH} + \text{H-CO-H} + \text{XO}_2 + \text{HO}_2$	5.9E-11	
179	Lp110	$7\text{OH-lim-CO-OH} + \text{O}_3 \rightarrow 0.84 \times (0.4 \times 7\text{OH-ketolim-CO-OH} + 0.4 \times \text{stab_limCIx-OO} + 0.2 \times (0.875 \times \text{keto-limononic_acid} + \text{CH}_3\text{-CO-OO} + \text{OH} + \text{XO}_2) + \text{H-CO-H}) + 0.16 \times (7\text{OH-ketolim-CO-OH} + [\text{.CH}_2\text{OO.}]^*)$	8.3E-18	
180	LH5_a	$\text{norlim-OOH} + \text{OH} \rightarrow 0.05 \times (\text{norlim-OO} + \text{H}_2\text{O}) + 0.95 \times (\text{nor-ketolim-OOH} + \text{H-CO-H} + \text{HO}_2 + \text{XO}_2)$	5.9E-11	
181	LH5_a1	$\text{norlim-OOH} + \text{O}_3 \rightarrow \text{nor-ketolim-OOH} + 0.2 \times [\text{.CH}_2\text{OO.}]^* +$	8.3E-18	

		$0.8 \times \text{H-CO-H} + 0.86 \times \text{OH}$		
182	Lp36	$\text{norlim} + \text{OH} \rightarrow 0.1 \times (\text{norlim-CO-OO} + \text{H}_2\text{O}) + 0.9 \times (\text{nor-ketolim} + \text{H-CO-H} + \text{HO}_2 + \text{XO}_2)$	$5.9\text{E-}11$	2
183	LO3P_5	$\text{norlim} + \text{O}_3 \rightarrow 1.125 \times \text{nor-ketolim}$	$2.5\text{E-}11$	
184	CI1_4add	$\text{norlim} + \text{O}_3 \rightarrow 0.84 \times (\text{C7-CHO} + \text{H-CO-H} + \text{XO}_2) + 0.16 \times (\text{ketolim} + [\text{.CH}_2\text{OO.}]^*) + 0.86 \times \text{OH}$	$8.3\text{E-}18$	
185	Lp38	$\text{norlim-CO-OO} + \text{HO}_2 \rightarrow 0.3 \times (\text{limononic_acid} + \text{O}_3) + 0.7 \times (\text{limonic_acid} + \text{O}_2)$	$2.86\text{E-}13 \times \text{EXP}(1250/\text{TK})$	3
186	Lp40	$\text{C=C7-OO} + \text{HO}_2 \rightarrow 0.6 \times (\text{C=C7-OOH} + \text{O}_2) + 0.4 \times (\text{C=C7} + \text{H}_2\text{O} + \text{O}_2)$	$2.8\text{E-}13 \times \text{EXP}(1250/\text{TK})$	3
187	Lp41	$\text{norlim-CO-OOH} + \text{OH} \rightarrow 0.9 \times (\text{nor-ketolim-CO-OOH} + \text{H-CO-H} + \text{XO}_2 + \text{OH}) + 0.1 \times (\text{norlim-CO-OO} + \text{H}_2\text{O})$	$5.9\text{E-}11$	
188	Lp41_a1	$\text{norlim-CO-OOH} + \text{O}_3 \rightarrow \text{nor-ketolim-CO-OOH} + 0.2 \times [\text{.CH}_2\text{OO.}]^* + 0.8 \times \text{H-CO-H} + 0.86 \times \text{OH}$	$8.3\text{E-}18$	
189	Lp103	$\text{oxy-lim} + \text{OH} \rightarrow 0.7 \times (\text{ketolim} + \text{H-CO-H} + \text{XO}_2 + \text{HO}_2) + 0.3 \times (\text{norlim-CO-OO} + \text{CO})$	$5.9\text{E-}11$	2
190	Lp104	$\text{oxy-lim} + \text{O}_3 \rightarrow 0.84 \times (\text{limCIx-OO}^* + \text{H-CO-H}) + 0.16 \times (\text{ketolim} + [\text{.CH}_2\text{OO.}]^*) + 0.86 \times \text{OH}$	$8.3\text{E-}18$	
191	Lp16	$\text{ketolim} + \text{OH} \rightarrow 0.9 \times (\text{ketolim-CO-OO} + \text{H}_2\text{O}) + 0.1 \times (0.5 \times (\text{H-CO-CO-H} + \text{C7}) + 0.5 \times (\text{C6-CHO} + \text{CH}_3\text{-CO-OO.} + \text{HO}_2 + \text{XO}_2) + \text{XO}_2 + \text{H}_2\text{O})$	$4.0\text{E-}11$	2
192	Lp19_a	$\text{ketolim-CO-OO} + \text{HO}_2 \rightarrow 0.3 \times (\text{keto-limononic_acid} + \text{O}_3) + 0.7 \times (\text{ketolim-CO-OOH} + \text{O}_2)$	$2.9\text{E-}13 \times \text{EXP}(1250/\text{TK})$	3
193	Lp35	$\text{ketolim-CO-OOH} + \text{OH} \rightarrow 0.9 \times (0.5 \times (\text{C7} + \text{H-CO-CO-OOH} + \text{XO}_2 + \text{HO}_2) + 0.5 \times (\text{C6-CO-OOH} + \text{CH}_3\text{-CO-OO.}) + \text{XO}_2) + 0.1 \times (\text{ketolim-CO-OO} + \text{H}_2\text{O})$	$1.4\text{e-}11$	2
194	Lp35a	$\text{ketolim-OH-iOOH} + \text{OH} \rightarrow \text{ketolim} + \text{H}_2\text{O} + \text{HO}_2 + \text{XO}_2$	$1.2\text{e-}12$	2
195	Lp27c	$\text{lim-XOH-OOH} + \text{OH} \rightarrow 0.3 \times (\text{ketolim} + 0.65 \times \text{H}_2\text{O} + 0.65 \times \text{XO}_2 + 0.35 \times \text{OH} + \text{H-CO-H} + \text{HO}_2) + 0.7 \times (\text{XOH-OOH-lim-CO-OO} + \text{H}_2\text{O})$	$2.0\text{e-}11$	
196	LY1_6	$\text{XOH-OOH-norlim} + \text{OH} \rightarrow 0.73 \times \text{XOH-OOH-norlim-CO-OO} + 0.27 \times (\text{nor-ketolim} + \text{H-CO-H}) + 0.14 \times \text{OH} + 0.13 \times \text{HO}_2 + \text{H}_2\text{O}$	$2.84\text{E-}11$	2
197	LY1_8	$\text{XOH-OOH-norlim-CO-OO} + \text{HO}_2 \rightarrow 0.7 \times (\text{XOH-OOH-norlim-CO-OOH} + \text{O}_2) + 0.3 \times (\text{XOH-OOH-norlim-CO-OH} + \text{O}_3)$	$2.86\text{E-}13 \times \text{EXP}(1250/\text{TK})$	3
198	Lp27g	$\text{XOH-OOH-lim-CO-OO} + \text{HO}_2 \rightarrow 0.7 \times (\text{XOH-OOH-lim-CO-OOH} + \text{O}_2) + 0.3 \times (\text{XOH-OOH-lim-CO-OH} + \text{O}_3)$	$2.9\text{E-}13 \times \text{EXP}(1250/\text{TK})$	3
199	Lp42	$\text{nor-ketolim-OOH} + \text{OH} \rightarrow \text{nor-ketolim-OO} + \text{H}_2\text{O}$	$1.2\text{e-}12$	2
200	Lp44	$\text{nor-ketolim-OO} + \text{HO}_2 \rightarrow 0.6 \times (\text{nor-ketolim-OOH} + \text{O}_2) + 0.4 \times (\text{nor-ketolim} + \text{O}_2 + \text{H}_2\text{O})$	$2.8\text{E-}13 \times \text{EXP}(1250/\text{TK})$	3
201	Lp45	$\text{nor-ketolim} + \text{OH} \rightarrow \text{nor-ketolim-CO-OO} + \text{H}_2\text{O}$	$2.3\text{E-}11$	
202	Lp47	$\text{nor-ketolim-CO-OO} + \text{HO}_2 \rightarrow 0.3 \times (\text{nor-ketolimonic_acid} + \text{O}_3) + 0.7 \times (\text{nor-ketolim-CO-OOH} + \text{O}_2)$	$2.8\text{E-}13 \times \text{EXP}(1250/\text{TK})$	3
203	Lp48	$\text{nor-ketolim-CO-OOH} + \text{OH} \rightarrow \text{nor-ketolim-CO-OO} + \text{H}_2\text{O}$	$1.2\text{e-}12$	2
204	Lp55	$\text{oxo_acid} + \text{OH} \rightarrow \text{keto-limononic_acid} + \text{HO}_2 + \text{H}_2\text{O}$	$11.5\text{E-}12$	
205	Lp57	$\text{keto-limonic_acid} + \text{OH} \rightarrow \text{keto-limonic_acid}$	$50.2\text{E-}12$	
206	Lp47_a	$2(\text{CHO-CH}_2)\text{-CH}(\text{CH}_3\text{-C}=\text{CH}_2) + \text{OH} \rightarrow 0.6 \times (0.857 \times \text{C7-CHO} + \text{H-CO-H} +$	$53.4\text{e-}12$	2

		$XO_2+HO_2)+0.4\times(C=C_5-CHO+CO_2+HO_2+2\times XO_2+H_2O)$		
207	Lp32_e	$2(CHO-CH_2)-CH-(CH_3-C=CH_2)+O_3\rightarrow 0.84\times(0.875\times C_7-CHO+XO_2+H-CO-H)+0.16\times(0.875\times C_7-CHO+[.CH_2OO.]^*)+0.86\times OH$	8.3E-18	
208	Lp49	$C=C_7+OH\rightarrow C_7+H-CO-H+XO_2+HO_2$	8.25E-11	2
209	Lp32_f	$C=C_7+O_3\rightarrow 0.16\times(C_7+[.CH_2OO.]^*+O_3)+0.84\times(C_7+H-CO-H+XO_2)+0.86\times OH$	8.3E-18	
210	LO3P_6	$C=C_7+O_3P\rightarrow 1.14\times C_7$	2.5E-11	
211	Lp40e	$oxy-C=C_7+OH\rightarrow C_6-CHO+H-CO-H+XO_2+HO_2$	2.3E-11	2
212	Lp40g	$oxy-C=C_7+O_3\rightarrow 0.84\times(C_6-CHO+H-CO-H)+0.16\times(C_6-CHO+[.CH_2OO.]^*)+0.86\times OH$	8.3E-18	
213	Lp40h	$oxy-C=C_7+O_3P\rightarrow C_7-CHO$	2.5E-11	
214	Lp29d	$C_7-CHO+OH\rightarrow C_6-CHO+H_2O+2\times XO_2+CO_2$	3E-11	
215	Lp49a	$C_6-CHO+OH\rightarrow 0.9\times(C_5-CHO+2\times XO_2+CO_2)+0.1\times(C_3+C_4+XO_2)$	2.31E-11	2
216	Lp1B	$MCH-OO+HO_2\rightarrow MCH-OOH+O_2$	$2.72E-13\times EXP(1250/TK)$	3
217	Lp1	$MCH=O+OH\rightarrow C_6-CHO+HO_2+XO_2$	9.44E-11	
218	Lp32_a	$MCH=O+O_3\rightarrow 0.65\times(0.25\times(C_5-CHO+CH_3-CO-OO.+XO_2))+0.35\times stab_MCHCI-CH_3-OO+0.05\times(C_6-CHO+O_3P)+0.35\times(C_5-CHO+CO_2))+0.35\times(0.2\times(C_5-CHO+HO_2+CO+XO_2))+0.3\times C_6-CO-OH+0.5\times stab_MCHCI-OO)+0.86\times OH$	1.8e-16	
219	Lp33	$MCH-CH_3+OH\rightarrow C_7-CHO+XO_2+HO_2$	6.77E-12	2
220	Lp32_b	$MCH-CH_3+O_3\rightarrow 0.65\times(0.25\times(C_5-CHO+CH_3-CO-OO.+XO_2))+0.35\times stab_MCHCI-CH_3-OO+0.05\times(C_6-CHO+O_3P)+0.35\times(C_5-CHO+CO_2))+0.35\times(0.2\times(C_5-CHO+HO_2+CO+XO_2))+0.3\times C_6-CO-OH+0.5\times stab_MCHCI-OO)+0.86\times OH$	1.8e-16	
		Partitioning reactions	S_b ($J\ mol^{-1}K^{-1}$), T_b (K)	
221	LGP10	$limonic_acid+seed\rightarrow part1+seed$	$S_{b_1} = 109.595, T_{b_1} = 567.45$	11, 12, 13, 14
222	LGP17	$lim-XO-OH+seed\rightarrow part8+seed$	$S_{b_8} = 112.22, T_{b_8} = 585.80$	
223	LGP19_1	$limonic_acid+seed\rightarrow part11+seed$	$S_{b_11} = 127.895, T_{b_11} = 610.34$	
224	LGP19_2	$7OH-lim-CO-OH+seed\rightarrow part12+seed$	$S_{b_12} = 129.045, T_{b_12} = 617.41$	
225	LGP19_3	$keto-limononic_acid+seed\rightarrow part13+seed$	$S_{b_13} = 112.495, T_{b_13} = 586.25$	
226	LGP19_4	$limononaldehyde+seed\rightarrow part14+seed$	$S_{b_14} = 92.595, T_{b_14} = 508.04$	
227	LGP19_5	$ketolim+seed\rightarrow part15+seed$	$S_{b_15} = 95.495, T_{b_15} = 531.03$	
228	LGP19_6	$7OH-lim+seed\rightarrow part16+seed$	$S_{b_16} = 112.495, T_{b_16} = 570.08$	
229	LGP19_7	$oxy-lim+seed\rightarrow part17+seed$	$S_{b_17} = 96.32, T_{b_17} =$	

			541.98	
230	LGP19_8	7OH-ketolim+seed→part18+seed	Sb_18 = 114.945, Tb_18 = 588.66	
231	LGP19_9	7OH-ketolim-CO-OH+seed→part19+seed	Sb_19 = 131.945, Tb_19 = 632.57	
232	LGP19_10	norlimononic_acid+seed→part20+seed	Sb_20 = 110.895, Tb_20 = 561.09	
233	LGP19_11	oxo_acid+seed→part21+seed	Sb_21 = 148.62 , Tb_21 = 644.20	
234	LGP19_13	keto-limononic_acid+seed→part23+seed	Sb_23 = 137.145, Tb_23 = 610.34	
235	LGP19_14	keto-limonalic_acid+seed→part24+seed	Sb_24 = 113.795, Tb_24 = 580.37	
236	LGP19_15	limonalic_acid+seed→part25+seed	Sb_25 = 110.895, Tb_25 = 561.09	
237	LGP20	limononic_acid→part1		
238	LGP27	lim-XO-OH→part8		
239	LGP29_1	limonic_acid→part11		
240	LGP29_2	7OH-lim-CO-OH→part12		
241	LGP29_3	keto-limononic_acid→part13		
242	LGP29_4	limononaldehyde→part14		
243	LGP29_5	ketolim→part15		
244	LGP29_6	7OH-lim→part16		
245	LGP29_7	oxy-lim→part17		
246	LGP29_8	7OH-ketolim→part18		
247	LGP29_9	7OH-ketolim-CO-OH→part19		
248	LGP29_10	norlimononic_acid→part20		
249	LGP29_11	oxo_acid→part21		
250	LGP29_13	keto-limononic_acid→part23		
251	LGP29_14	keto-limonalic_acid→part24		
252	LGP29_15	limonalic_acid→part25		
			Ea/R (K)	
253	LGP0off	part1→limononic_acid	EaR_1=9207.1	15
254	LGP7off	part8→lim-XO-OH	EaR_8=9411.2	
255	LGP10off	part11→limonic_acid	EaR_11=9958.7	
256	LGP11off	part12→7OH-lim-CO-OH	EaR_12=10053.9	
257	LGP12off	part13→keto-limononic_acid	EaR_13=9420.4	
258	LGP13off	part14→limononaldehyde	EaR_14=8489.6	
259	LGP14off	part15→ketolim	EaR_15=8690.8	
260	LGP15off	part16→7OH-lim	EaR_16=9273.9	
261	LGP16off	part17→oxy-lim	EaR_17=8781.8	

262	LGP17off	part18→7OH-ketolim	EaR_18=9489.6	
263	LGP18off	part19→7OH-ketolim-CO-OH	EaR_19=10273.2	
264	LGP19off	part20→norlimononic_acid	EaR_20=9101.5	
265	LGP20off	part21→oxo_acid	EaR_21=10794.5	
266	LGP22off	part23→keto-limononic_acid	EaR_23=10184.3	
267	LGP23off	part24→keto-limonalic_acid	EaR_24=9394.9	
268	LGP24off	part25→limonalic_acid	EaR_25=9177.5	
		Particle phase reactions	sec ⁻¹ or cm ³ molecule ⁻¹ sec ⁻¹	
269	LGP14poly	part14+seed→part14s+seed	0.5e-14	
270	LGP15poly	part15+seed→part15s+seed	0.5e-14	
271	LGP1poly	part1+seed→part1s+seed	0.5e-14	
272	LGP9poly	part9+seed→part9s+seed	0.5e-14	
273	LGP17poly	part17+seed→part17s+seed	0.5e-14	
274	LGP13poly	part13+seed→part13s+seed	0.5e-14	
275	LGP14polyr	part14s→part14	0.0001	
276	LGP15polyr	part15s→part15	0.0001	
277	LGP1polyr	part1s→part1 0.0001		
278	LGP9polyr	part9s→part9 0.0001		
279	LGP17polyr	part17s→part17	0.0001	
280	LGP13polyr	part13s→part13	0.0001	
281	LGP25polyr	part15s→part25	0.0001	
		Losses		
282	LGP0dep	seed→	1.33E-05	
283	LGP1dep	part1→	1.33E-05	
284	LGP8dep	part8→	1.33E-05	
285	LGP11dep	part11→	1.33E-05	
286	LGP12dep	part12→	1.33E-05	
287	LGP13dep	part13→	1.33E-05	
288	LGP14dep	part14→	1.33E-05	
289	LGP15dep	part15→	1.33E-05	
290	LGP16dep	part16→	1.33E-05	
291	LGP17dep	part17→	1.33E-05	
292	LGP18dep	part18→	1.33E-05	
293	LGP19dep	part19→	1.33E-05	
294	LGP20dep	part20→	1.33E-05	
295	LGP21dep	part21→	1.33E-05	
296	LGP22dep	part22→	1.33E-05	
297	LGP23dep	part23→	1.33E-05	
298	LGP24dep	part24→	1.33E-05	
299	LGP25dep	part25→	1.33E-05	

300	LGP1sdep	part1s→	1.33E-05	
301	LGP9sdep	part9s→	1.33E-05	
302	LGP14sdep	part14s→	1.33E-05	
303	LGP15sdep	part15s→	1.33E-05	
304	LGP17sdep	part17s→	1.33E-05	
305	O3_part	O3→	3.0E-18	
306	DepoH2O2	H2O2→	6.7E-4	
307	DepoO3	O3→	2.3E-6	
		Operator reactions		
308	XO_3	XO2+XO2→	2.5E-13*EXP(190/TK)	16
309	XO_4	XO2+HO2→	3.8E-13*EXP(800/TK)	16

Literature Cited

- (1) Atkinson, R. *Journal of Physical and Chemical Reference Data* **1997**, 26, 215-290.
- (2) Kwok, E. S. C.; Atkinson, R. *Atmospheric Environment* **1995**, 29, 1685-95.
- (3) Jenkin, M. E.; Saunders, S. M.; Pilling, M. J. *Atmospheric Environment* **1997**, 31, 81-104.
- (4) Luo, D.; Pierce, J. A.; Malkina, I. L.; Carter, W. P. L. *International Journal of Chemical Kinetics* **1996**, 28, 1-8.
- (5) Khamaganov, V. G.; Hites, R. A. *Journal of Physical Chemistry A* **2001**, 105, 815-822.
- (6) Shu, Y.; Atkinson, R. *International Journal of Chemical Kinetics* **1994**, 26, 1193-205.
- (7) Finlayson-Pitts, B. J. and Pitts, J. N. *Chemistry of the Upper and Lower Atmosphere: Theory, Experiments, and Applications*. 1040 pp. 1999.
- (8) Becker, K. H.; Bechara, J.; Brockmann, K. J. *Atmospheric Environment, Part A: General Topics* **1993**, 27A, 57-61.
- (9) Kamens, R.; Jang, M.; Chien, C.-J.; Leach, K. *Environmental Science and Technology* **1999**, 33, 1430-1438.
- (10) Neeb, P.; Horie, O.; Moortgat, G. K. *Tetrahedron Letters* **1996**, 37, 9297-9300.

- (11) Pankow, J. F. *Atmospheric Environment* **1994**, 28, 189-93.
- (12) Mackay, D.; Bobra, A.; Chan, D. W.; Shiu, W. Y. *Environ. Sci. Technol.* **1982**, 16 645-649.
- (13) Joback, K. G.; Reid, R. C. *Chem. Eng. Commun.* **1987**, 57 (1-6), 233-243.
- (14) Stein, S. E.; Brown, R. L. *J.Chem. Inf. Comput. Sci.* **1994**, 34 581-587.
- (15) Zhao, L.; Li, P.; Yalkowsky, S. H. *Journal of Chemical Information and Computer Sciences.* **1999**, 39 1112-1116.
- (16) Adelman Z. E. University of North Carolina at Chapel Hill, 1999.